ELSEVIER

Biochimica et Biophysica Acta 1507 (2001) 5–31

BIOCHIMICA ET BIOPHYSICA ACTA
BBA

www.bba-direct.com

Review

Structure of photosystem I

Petra Fromme [a,c,*], Patrick Jordan [b], Norbert Krauß [b,1]

[a] *Max Volmer Laboratorium für Biophysikalische Chemie Institut für Chemie, Technische Universität Berlin, Straße des 17 Juni 135, D-10623 Berlin, Germany*

[b] *Institut für Chemie/Kristallographie, Freie Universität Berlin, Takustraße 6, D-14195 Berlin, Germany*

[c] *Department of Chemistry and Biochemistry, Arizona State University, Tempe, AZ 85287-1604, USA*

Received 11 December 2000; received in revised form 4 July 2001; accepted 5 July 2001

Abstract

In plants and cyanobacteria, the primary step in oxygenic photosynthesis, the light induced charge separation, is driven by two large membrane intrinsic protein complexes, the photosystems I and II. Photosystem I catalyses the light driven electron transfer from plastocyanin/cytochrome c_6 on the lumenal side of the membrane to ferredoxin/flavodoxin at the stromal side by a chain of electron carriers. Photosystem I of *Synechococcus elongatus* consists of 12 protein subunits, 96 chlorophyll *a* molecules, 22 carotenoids, three [4Fe4S] clusters and two phylloquinones. Furthermore, it has been discovered that four lipids are intrinsic components of photosystem I. Photosystem I exists as a trimer in the native membrane with a molecular mass of 1068 kDa for the whole complex. The X-ray structure of photosystem I at a resolution of 2.5 Å shows the location of the individual subunits and cofactors and provides new information on the protein–cofactor interactions. [P. Jordan, P. Fromme, H.T. Witt, O. Klukas, W. Saenger, N. Krauß, Nature 411 (2001) 909-917]. In this review, biochemical data and results of biophysical investigations are discussed with respect to the X-ray crystallographic structure in order to give an overview of the structure and function of this large membrane protein.

Keywords: X-ray crystallography; Photosystem I; Structure; Electron transfer chain; Core antenna; Membrane protein

1. Introduction

Life on earth depends upon the process of oxygenic photosynthesis, using the light energy from the sun to convert CO_2 into carbohydrates. In plants and cyanobacteria, the latter producing about 30% of the total oxygen in the atmosphere, two photosystems, I and II, catalyse the first step of this conversion, the light induced transmembrane charge separation. In both photosystems, the energy of photons from sun light is used to translocate electrons across the thylakoid membrane via a chain of electron carriers. Water, oxidised to O_2 and $4H^+$ by photosystem II, acts as electron donor for the whole process. The

Abbreviations: Chl, chlorophyll; EPR, electron paramagnetic resonance; ENDOR, electron nuclear double resonance; ETC, electron transfer chain; FNR, ferredoxin-NADP$^+$-oxidoreductase; F_X, F_A and F_B, [4Fe4S] clusters of photosystem I; LHC, light harvesting complex; P700, primary electron donor of PS I; PS I, photosystem I; PS II, photosystem II; A_0, spectroscopically identified primary electron acceptor in PS I; A_1, spectroscopically identified secondary electron acceptor in PS I; RC, reaction centre; PbRC, purple bacterial photosynthetic reaction centre

* Corresponding author. Fax: +49-30-314-21122.

E-mail addresses: fromme@phosis1.chem.tu-berlin.de (P. Fromme), norbert.krauss@charite.de (N. Krauß).

[1] Also corresponding author. Present address: Institut für Biochemie, Universitätsklinikum Charité, Medizinische Fakultät der Humboldt Universität zu Berlin, Monbijoustraße 2, D-10117 Berlin, Germany. Fax +49-30-450-528-942

0005-2728/01/$ – see front matter
PII: S0005-2728(01)00195-5

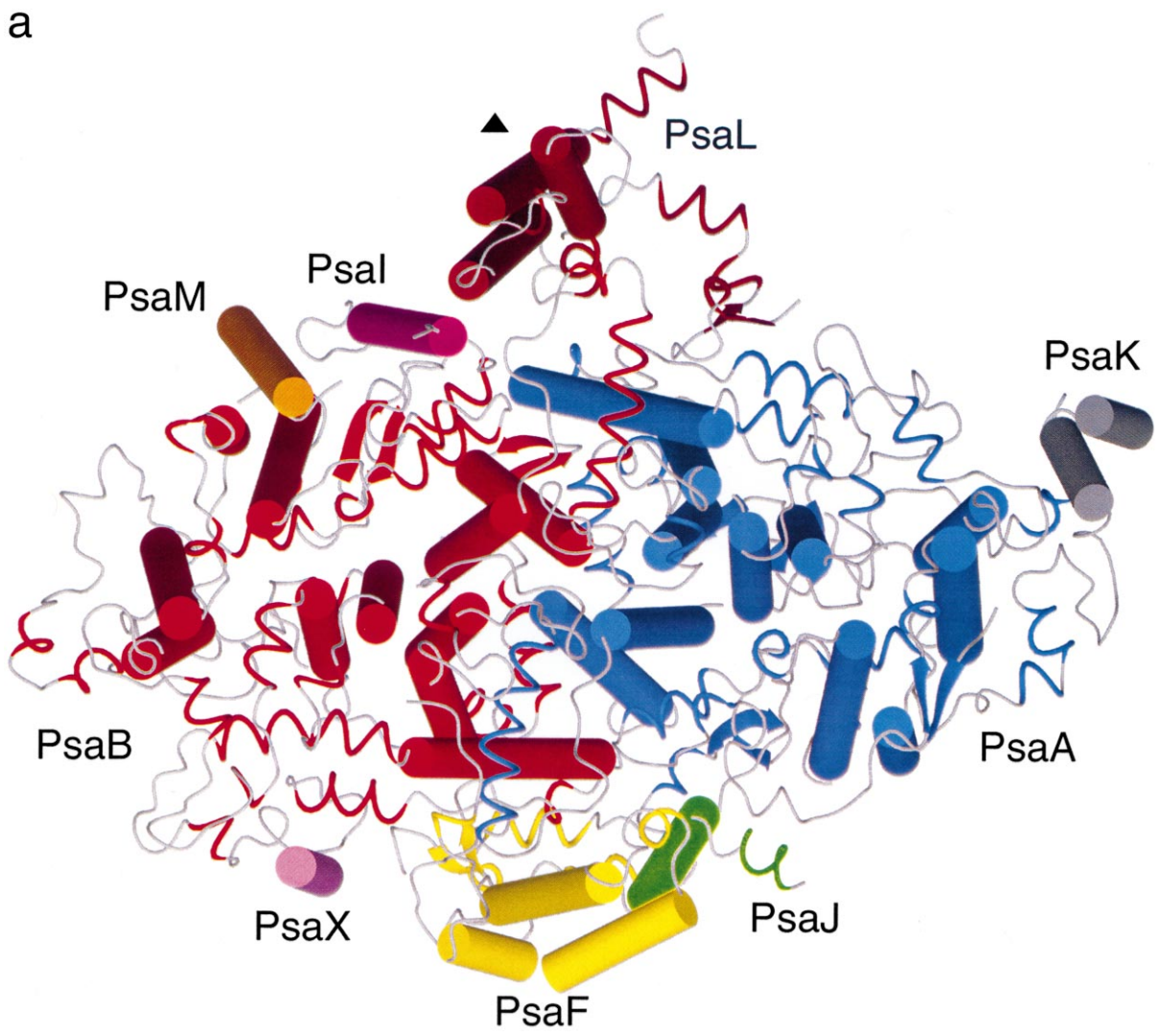

Fig. 1. Arrangement of protein subunits and cofactors in one monomeric unit of photosystem I. (a) and (b) View from the stromal side onto the membrane plane along the crystallographic three-fold axis (indicated by a black triangle). The three stromal subunits have been omitted for clarity. Colour coding of the membrane intrinsic subunits is as follows: PsaA, blue; PsaB, red; PsaF, yellow; PsaI, dark pink; PsaJ, green; PsaK, grey; PsaL, brown; PsaM, orange; and PsaX, light pink. In (a) and (b) transmembrane α-helices of the membrane intrinsic subunits are represented as coloured cylinders. (a) Ribbon representation of the extra-membraneous parts of the structure, loops coloured grey. (b) The transmembrane α-helices of the protein and the cofactors of the complex. Transmembrane α-helices of the subunits PsaF, PsaK and PsaL are labelled according to the nomenclature introduced in Jordan et al. [3]. Transmembrane α-helices of PsaA and PsaB are labelled by single letters, e.g. the blue cylinder 'a' represents the transmembrane α-helix A-a. Organic cofactors of the ETC are shown in blue, the [4Fe4S] clusters in orange/yellow. Chlorophylls are coloured yellow, carotenoids black and the lipids cyan.

two photosystems, which are coupled by a plastoquinone pool, the cytochrome b_6f complex and the soluble electron carrier proteins plastocyanin or cytochrome c_6 operate in series. The electron transfer processes are coupled to a build up of a difference in proton concentration across the thylakoid membrane. The resulting electrochemical membrane potential drives the synthesis of ATP from ADP and inorganic phosphate, catalysed by the ATP-synthase. Finally, photosystem I reduces ferredoxin, providing the electrons for the reduction of $NADP^+$ to NADPH by ferredoxin-$NADP^+$-oxidoreductase (FNR). NADPH and ATP are used to reduce CO_2 to carbohydrates in the subsequent dark reactions.

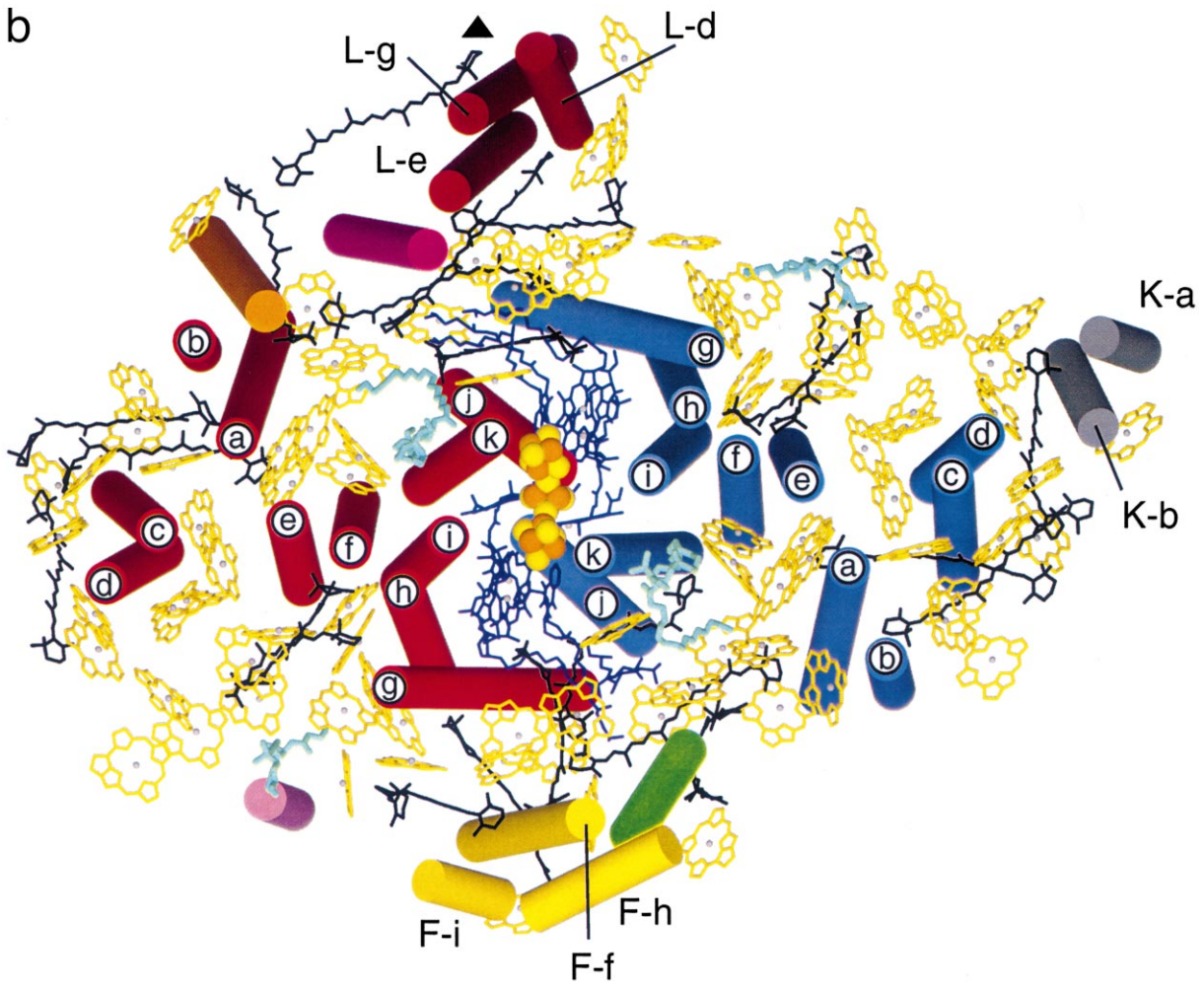

Fig. 1 (*continued*).

Photosystem I is a large multi-subunit protein complex, embedded into the photosynthetic thylakoid membrane. It catalyses the light induced electron transfer from plastocyanin or cytochrome c_6 on the lumenal side of the membrane (inside the thylakoids) to ferredoxin or flavodoxin on the stromal side of the membrane. Photosystem I consists of 12 (in cyanobacteria), or 13 (in plant systems) individual proteins. The subunits are named according to their genes PsaA to PsaX (for review on photosystem I see [1,2]). Photosystem I from the thermophilic cyanobacterium *Synechococcus elongatus* contains 96 chlorophyll (Chl) *a* molecules, 22 carotenoids, three [4Fe4S] clusters and two phylloquinones. In the recent X-ray structure at 2.5 Å resolution [3] four lipids were also identified. In cyanobacteria, photosystem I is present most dominantly in vivo in trimeric form [4]. A large number of the cofactors present in photosystem I are involved in the processes of light capturing, charge separation and prevention of photodamage.

The light is captured by a large core antenna system consisting of 90 Chl*a* molecules and 22 carotenoids. In plants a membrane integral antenna system (light harvesting complex (LHCI)) is also closely associated with photosystem I. The excitation energy is transferred from the antenna pigments to the primary electron donor P700. It was already proposed in the 1960s, that P700 is a dimer of chlorophyll molecules [5,6], and this is confirmed by the recent X-ray structure analysis [3]. The excitation energy is used to build up the singlet excited state P700*, lead-

ing to charge separation, where $P700^{+\bullet}$ remains and the electron is transferred across the thylakoid membrane by a chain of electron carriers. This process of transmembrane charge separation was intensively investigated spectroscopically (for review on electron transfer in photosystem I see [7]), whereby five different electron acceptors have been identified: A_0 (Chl*a* molecule), A_1 (phylloquinone), and the three [4Fe4S] clusters F_X, F_A and F_B. The electron is transferred from the terminal FeS cluster to the soluble electron carrier ferredoxin. In the case of iron deficiency, flavodoxin acts as a mobile electron carrier. $P700^{+\bullet}$ is finally rereduced by the soluble electron carrier plastocyanin; in cyanobacteria cytochrome c_6 can also act as an electron donor to photosystem I.

Photosystem I belongs to a larger group of protein–pigment complexes which are able to perform light induced charge separation: the photosynthetic reaction centres (RCs). These can be divided into two classes defined by the nature of the terminal electron acceptor. A quinone molecule is the terminal electron acceptor in type II reaction centres (quinone type reaction centre), which include the photosystem II reaction centre and the reaction centres of purple bacteria. In type I reaction centres, such as the photosystem I reaction centre described here, the terminal electron acceptor is an [4Fe4S] cluster (FeS type reaction centre). The photosynthetic reaction centres of the green sulfur bacteria and the heliobacteria [8,9] are also type I reaction centres. There is structural evidence that all photosynthetic reaction centres have evolved from a common ancestor [10], despite the large differences between photosystems of the same group in structure (for example protein and chromophore composition), as well as in function (for example redox potential, chemical nature of the electron donor to the reaction centre).

In 1993, the first structural model of photosystem I at 6 Å resolution was published, and later improved to 4 Å [11–15]. These models provide a first overview on the structure. Recently, the structure of photosystem I was determined at 2.5 Å resolution [3], providing for the first time detailed insights into the molecular architecture of this complex. The structure contains the models of the protein subunits and the 127 cofactors, (96 Chl*a*, 22 carotenoids, two phylloquinones, three [4Fe4S] clusters and four lipids). For these cofactors, details concerning their structure,

Table 1
The PS I subunits

Subunit	Location[a]	Interaction with ETC cofactors, antenna chlorophylls and carotenoid clusters
PsaA	membrane intrinsic, central	ETC: eC-A1, eC-A2, eC-A3, Q_K-A, F_X antenna chlorophylls: 40 carotenoid cluster: (1), (3), (5), (6)
PsaB	membrane intrinsic, central	ETC: eC-B1, eC-B2, eC-B3, Q_K-B, F_X antenna chlorophylls: 39 carotenoid cluster: (2), (4), (5), (6)
PsaC	stromal, central	ETC: F_A, F_B
PsaD	stromal, proximal	
PsaE	stromal, distal	
PsaF	membrane intrinsic, distal	carotenoid cluster: (5)
PsaI	membrane intrinsic, proximal	carotenoid cluster: (6)
PsaJ	membrane intrinsic, distal	antenna chlorophylls: 3 carotenoid cluster: (5)
PsaK	membrane intrinsic, peripheral	antenna chlorophylls: 2 carotenoid cluster: (1)
PsaL	membrane intrinsic, proximal	antenna chlorophylls: 3 carotenoid cluster: (6)
PsaM	membrane intrinsic, proximal	antenna chlorophylls: 1 carotenoid cluster: (6)
PsaX	membrane intrinsic, distal	antenna chlorophylls: 1

[a]Proximal and distal refer to the location with respect to the C_3 symmetry axis of the PS I trimer, central is close to the pseudo-C_2 axis of the PsaA/PsaB heterodimer.

orientation as well as interactions with the protein subunits and other cofactors are unravelled. In this review, the new structural model is discussed with respect to present knowledge about the function of photosystem I.

2. The architecture and function of protein subunits in photosystem I

2.1. General architecture

In the crystalline state as well as in vivo, photosystem I from the thermophilic cyanobacterium *S. elongatus* occurs as trimer [4,11]. The trimer has a diameter of 210 Å and a maximal height of 90 Å.

The location of the individual subunits in the cyanobacterial photosystem I is shown in Fig. 1. Table 1 summarises the location and chromophore binding of the 12 individual subunits of photosystem I.

The central part of one monomeric unit of the photosystem I trimer is formed by a heterodimer, consisting of the large membrane intrinsic subunits PsaA and PsaB. These subunits are related by a local pseudo-C_2 symmetry axis. The components of the electron transfer chain (ETC) from P700 to F_X (consisting of six chlorophylls, two phylloquinones and the first [4Fe4S] cluster) are coordinated by PsaA and PsaB and located along the local pseudo-C_2 axis. The electron transfer chain is surrounded by the five C-terminal transmembrane α-helices each of PsaA and PsaB (A/B-g to A/B-k) forming the central core, whereas the six N-terminal transmembrane α-helices, each of PsaA and PsaB are arranged in form as a 'trimer of dimers'. Four of these 12 α-helices, A/B-e and A/B-f, are closely attached to the C-terminal central core. The antenna pigments of photosystem I (90 chlorophylls and 22 carotenoids) can be divided into a region, where the antenna pigments surround the inner core and two peripheral regions, close to the eight N-terminal transmembrane α-helices (A/B-a to A/B-d) of PsaA and PsaB. These α-helices and the small membrane intrinsic subunits of photosystem I are peripherally attached to the central core. PsaF, PsaJ and PsaX are located at the detergent exposed side, distal to the trimer axis. The N-terminal domain of PsaF is exposed to the lumenal side of the membrane.

PsaL is located close to the trimer axis, forming most of the contacts between adjacent monomers within the photosystem (PS) I trimer. PsaI and PsaM are also located at this 'inner' side of photosystem I. PsaK is well separated from the other small membrane intrinsic subunits and is only in contact with PsaA.

The subunits PsaC, PsaD and PsaE do not contain transmembrane α-helices (see Fig. 2). They are located on the stromal side of the complex, forming the stromal hump. They are in close contact to the stromal loop regions of PsaA and PsaB. Subunit PsaC carries the two terminal FeS clusters F_A and F_B, and is located in the central part of the stromal hump. PsaD forms the part of this hump, which is closest to the trimeric axis. The C-terminal part of PsaD forms a 'clamp' surrounding PsaC. PsaE is located on the side of the hump, which is distal from the trimer axis.

3. The two large subunits PsaA and PsaB

The major subunits of photosystem I, PsaA and PsaB, show strong sequence homology [16,17] and it was suggested that they have been evolved via gene duplication [8,18]. They form the central part of photosystem I. Both subunits contain 11 transmembrane helices (A/B-a to A/B-k) in agreement with predictions from hydrophobicity plots and the previous models of photosystem I at 4 Å resolution [12–15]. The sequential order of the transmembrane α-helices proposed in the last 4 Å model [14] is confirmed, nevertheless the helices have to be renamed in the structure at 2.5 Å resolution [3]. At low resolution, an assignment of PsaA and PsaB to each set of the 11 transmembrane α-helices was not possible, and the α-helices were thus labelled by primed and unprimed letters. Biochemical studies using protease digestion experiments were undertaken in the native PS I complex and in PS I deletion mutants of the stromal subunits. In these studies, sequence specific antibodies were used to assign the subunits PsaA and PsaB, with contradictory results [19,20]. The 2.5 Å structure reveals that the α-helices denoted as primed in the previous medium resolution structural models belong to subunit PsaB and the unprimed α-helices to PsaA. The N-termini of both subunits are stro-

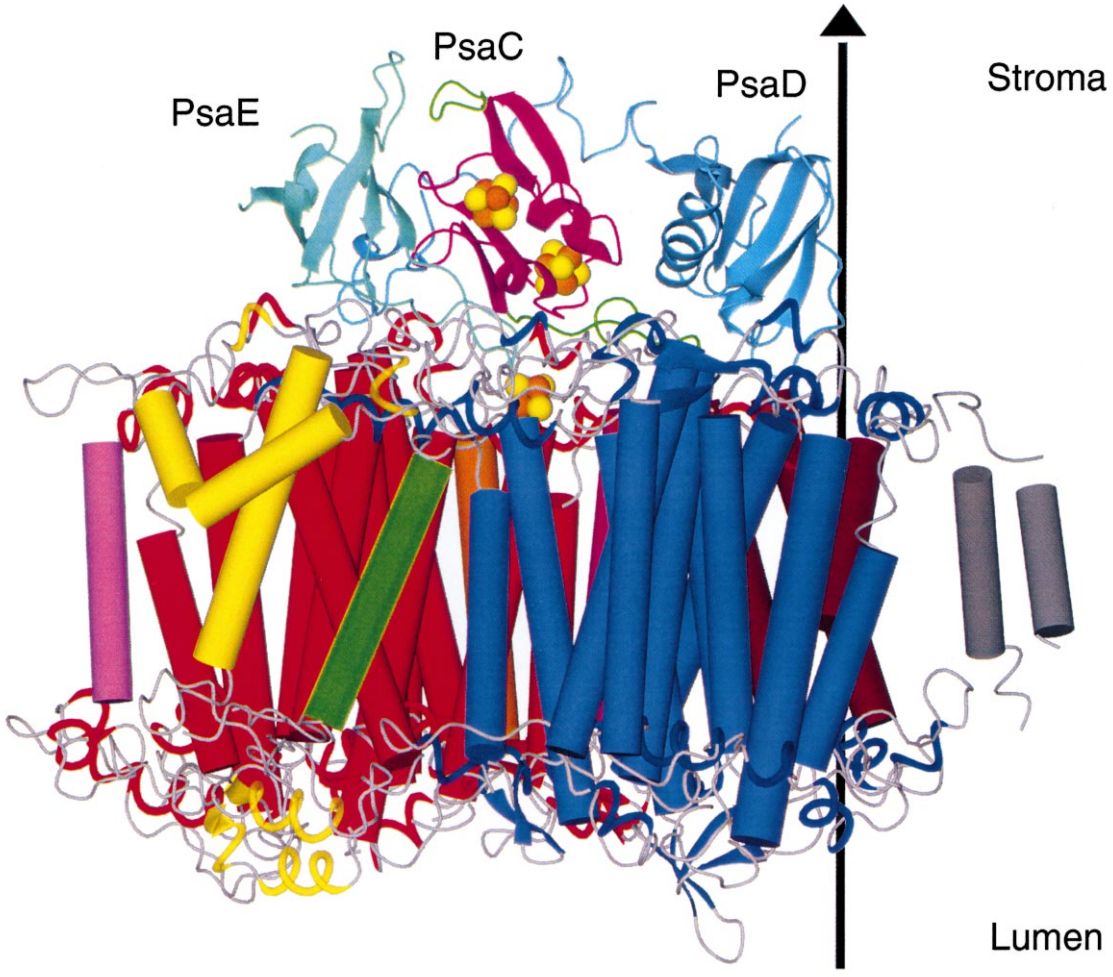

Fig. 2. Side view of the monomer of the PS I complex. View direction parallel to the membrane plane. For colours see legend to Fig. 1. The crystallographic three-fold axis (C_3) is indicated by the black vertical line. The three stromal subunits PsaE (light green), PsaC (violet) and PsaD (light blue) are located on top of the transmembrane α-helices. Structural regions corresponding to insertions in PsaC with respect to bacterial ferredoxins (see text) are coloured green.

mally exposed, as predicted from experiments using sequence specific antibodies [19], whereas the C-terminus is located on the lumenal side. The local pseudo-C_2 symmetry, which relates PsaA to PsaB is well preserved in the membrane integral parts, whereas large differences between the two subunits are visible in the loop regions. The loop regions are named according to the transmembrane α-helices, which they connect. Most of the loop regions contain secondary structure elements as α-helices and β-sheets. The loop regions on the lumenal side are generally more extended than the loops on the stromal side.

3.1. Membrane intrinsic part of PsaA and PsaB

The five C-terminal transmembrane α-helices A/B-g to A/B-k surround the electron transfer chain. This region structurally separates the electron transfer system from the antenna pigments of PS I. Of the six N-terminal α-helices (A/B-a to A/B-f), the pairs of α-helices A/B-e and A/B-f are closely attached to the five C-terminal transmembrane α-helices. Hydrophobic contacts are pronounced between α-helices A/B-e to A/B-k, whereas α-helices A/B-a to A/B-d are separated from the core by a $\approx$17 Å wide elliptical belt surrounding this inner core, which contains only

chlorophyll and carotenoid molecules. The C-terminal region of PsaA/PsaB was called the reaction centre domain [10,18], because it coordinates most of the cofactors of the electron transport chain and shows structural homologies to the RC core subunits L and M in the PbRC as well as to the RC core subunits D1 and D2 in photosystem II [10,21–23]. In contrast to these type II reaction centres, where the RC subunits do not bind chromophores of the antenna system, the C-terminal domains of PsaA and PsaB not only bind the cofactors of the electron transfer chain, but are also involved in the coordination of 25 chlorophylls of the antenna system (12 in PsaA and 13 in PsaB). The N-terminal domains of PsaA and PsaB, defined by the 12 α-helices A/B-a to A/B-f, coordinate 54 chlorophylls (28 in PsaA and 26 in PsaB). Another remarkable and unexpected feature of the photosystem I structure is that the chlorophylls are not exclusively coordinated by amino acid residues in the transmembrane α-helices. Of the 79 antenna chlorophylls coordinated by PsaA and PsaB only 48 are bound by the transmembrane helices, whereas 30 antenna chlorophylls are coordinated by amino acid side chains located in the loop regions.

Lipids have been biochemically detected in PS I core complexes consisting exclusively of PsaA and PsaB [24]. However, it was open to discussion as to whether they are intrinsic compounds of photosystem I or are located in the detergent micelle. The 2.5 Å structure shows that indeed four lipids are an essential part of photosystem I. Instead of being located close to the detergent exposed side of photosystem I, they are located in the core of PsaA and PsaB at positions following the local pseudo-C_2 symmetry of PsaA and PsaB.

3.2. The lumenal surface/docking site for cytochrome c_6

Loop regions of the subunits PsaA and PsaB form most of the lumenal surface of photosystem I. In addition, the N-terminal domain of PsaF, containing the two hydrophilic α-helices F-c and F-d, is located at this surface of PS I. However, these helices are too far away from the putative docking site of the soluble electron carriers cytochrome c_6 and plastocyanin to be directly involved in the electron transfer or the interaction with these electron carrier proteins. This is in good agreement with biochemical and mutagenesis studies, showing that PsaF is not involved in the docking process in cyanobacteria [25,26]. In contrast to cyanobacteria, the direct involvement of PsaF in docking has been shown for plant photosystem I ([27] and references therein). The difference in function can be explained by a part of the sequence, which is unique to plants. This view is confirmed by recent results of Hippler et al. [28], where a chimeric PsaF containing the C-terminal region of *S. elongatus* and the N-terminal region of *Chlamydomonas rheinhardtii* was introduced into *S. elongatus* photosystem I. The authors show that this leads to a PS I complex showing features of plastocyanin binding and rates of ET to $P700^+$ identical with that of *C. rheinhardtii* (for detailed discussion on the function of PsaF in cyanobacteria see below).

The putative binding pocket for the soluble electron carriers is centred on the local pseudo-two-fold axis and is a 10 Å deep hollow. The binding pocket is located at the same site as suggested from the model of photosystem I at 6 Å resolution [18]. Details of the docking site are now visible in the 2.5 Å structure. It is mainly formed by the loop regions A/B-ij, with α-helices A/B-ij(2) located at the bottom. These two α-helices had already been found at low resolution (named n and n′ in the 6 Å and 1/1′ in the 4 Å model [11,12]), and involvement in the interaction with plastocyanin had already been suggested [18], although sequence assignment was not yet possible. These α-helices consist of the segments IleA646 to SerA664 in PsaA and of TyrB621 to AsnB639 in PsaB. Two tryptophan residues, TrpA655 and TrpB631, are located in these α-helices such that they point into the binding pocket. This suggests a possible role of their aromatic side chains in the interaction of PS I with cytochrome c_6 and plastocyanin. Furthermore, it can be speculated whether they could be involved in electron transfer from these bound electron donor proteins to the oxidised primary donor $P700^{+\bullet}$. The interaction of the two α-helices A/B-ij(2) with cytochrome c_6 and plastocyanin is supported by mutagenesis studies of cyanobacterial PS I, which show that the electron transfer from cytochrome c_6 to PS I is affected if some of the amino acids in the helices A/B-ij(2) were substituted by cysteines [29]. However, an essential role of

the tryptophans in electron transfer has not yet been shown.

Large differences between PsaA and PsaB in sequence as well as in the secondary structure elements are found in the stromal N-terminal loop region as well as in the lumenal long loops A/B-ab, A/B-cd and A/B-gh.

3.3. The stromal loop regions of PsaA and PsaB

In general, most of the stromal loops are smaller than the lumenal loops. There is a relatively high degree of structural similarity, which includes the hydrophilic α-helices, between the two subunits PsaA and PsaB in the stromal loop regions. Most of the stromal loops of PsaA/B are in contact with the stromal subunits PsaC, PsaD and PsaE. The loop regions A/B-hi are very important for the function of photosystem I. Here, the conserved cysteine residues (CysA578, CysA587 and CysB565, CysB574) coordinate the iron sulfur centre F_X (see Fig. 8). Loop regions A/B-jk, which provide the binding sites of the phylloquinone cofactors with conserved TrpA697 and TrpB677 are also vital (details see below).

In retrospective, a great deal of biochemical data are confirmed by the 2.5 Å structure, examples being: the stromal loops connecting hydrophobic stretches X and XI of the subunits PsaA and PsaB (corresponding to helices A/B-j and A/B-k in the 2.5 Å structure) are protected against proteolysis in the presence of the stromal subunits PsaC, PsaD, and PsaE, but can be cleaved when these subunits are removed by chaotropic agents [30]; the stromal loop region B-jk, which includes the α-helix B-jk(1) (formerly named n′) is in close contact with PsaD and is therefore protected against proteolytic digestion as observed previously [20]. Furthermore, a higher accessibility for thermolysin was found for PsaB in mutants lacking PsaF and PsaJ [26] leading to proteolytic digestion in the lumenal loop region B-gh, which in fact is in contact to PsaF and additionally to PsaX.

4. The stromal subunits PsaC, PsaD and PsaE

Three subunits (PsaC, PsaD and PsaE) do not contain transmembrane α-helices (see Figs. 2 and 3). They are located on the stromal side of photosystem I and are involved in the docking of ferredoxin or flavodoxin.

4.1. Subunit PsaC

Subunit PsaC (8.9 kDa) carries the two terminal FeS clusters F_A and F_B. The clusters are characterised by their distinct electron paramagnetic resonance (EPR) spectra [31,32]. The role of subunit PsaC in coordination of the two terminal FeS clusters was suggested from the conserved sequence motif CXXCXXCXXXCP which is found twice in the gene of PsaC [33]. A homology of subunit PsaC to bacterial ferredoxins, also containing two [4Fe4S] clusters, was proposed from sequence similarity [34]. The structures of PsaC and these ferredoxins, such as that from *Peptostreptococcus asacharolyticus* [35], are indeed similar, with pronounced pseudo-two-fold symmetry, confirming previous models which related the structure of subunit PsaC to this ferredoxin [36]. The prominent deviations between the two structures are the C- and N-termini, elongated by 14 and two residues in PsaC, respectively, and an extension of 10 residues pointing towards the putative ferredoxin/flavodoxin docking site in the internal loop region exposed to the stromal surface of the PS I complex (coloured green in Figs. 2 and 3). The C-terminus of PsaC forms various interactions with PsaA/B and PsaD. This region seems to be important for the proper assembly of PsaC into the PS I complex.

A frequently asked question is whether F_A or F_B is the terminal FeS cluster which transfers the electron to ferredoxin. This has now been answered using results of EPR and mutagenesis studies in *Synechocystis* sp. *PCC6803*, which assigned the cysteine residues 21, 48, 51 and 54 to the cluster F_A and the cysteine residues 11, 14, 17 and 58 to the cluster F_B [37,38]. The structure shows that the cluster located at a centre to centre distance of 14.9 Å to F_X is F_A, and the second at a distance of 22 Å to F_X is F_B. A sequential electron transport from F_X to F_A to F_B is therefore most likely, in agreement with a large number of recent spectroscopic and biochemical studies ([39–41] and references therein).

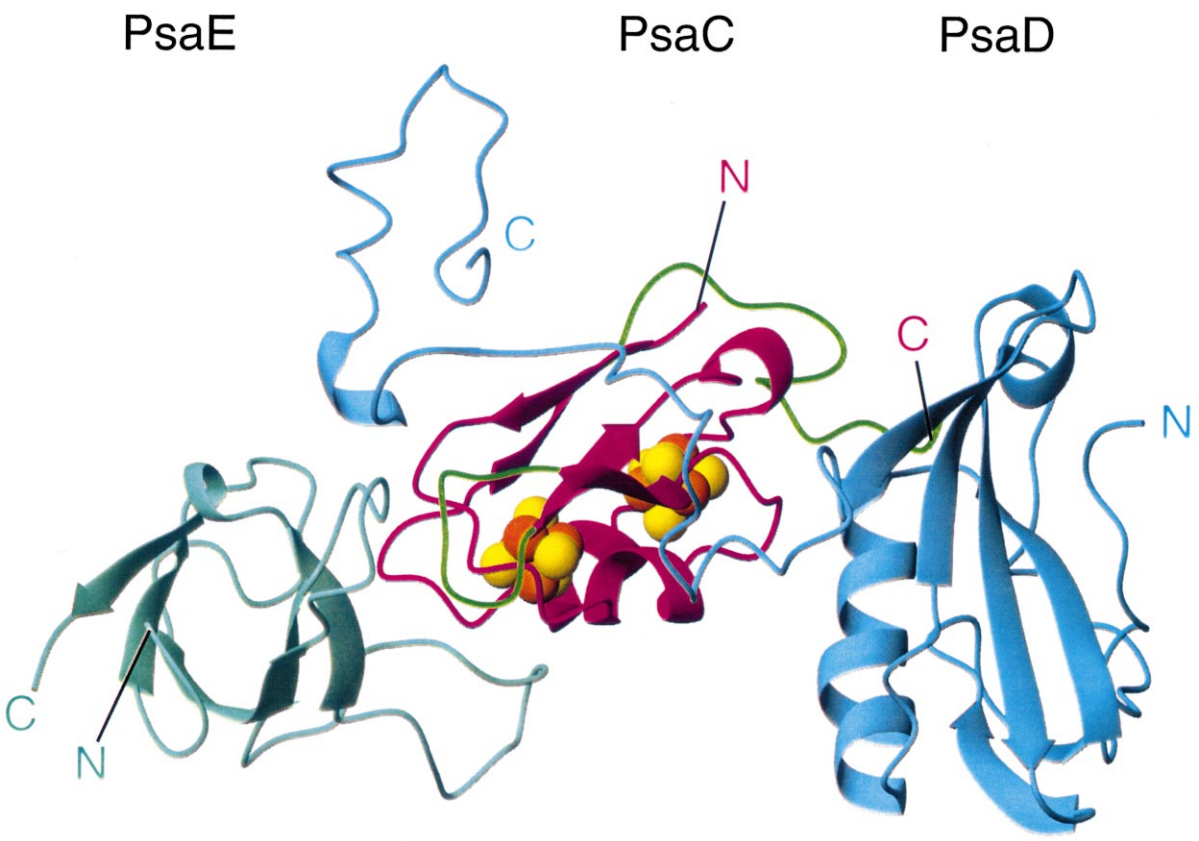

Fig. 3. Detailed view of the stromal subunits PsaC, PsaD and PsaE. View direction from the stromal side of the PS I complex onto membrane plane. The colours for the stromal subunits are chosen as in Fig. 2. N- and C-termini of the subunits are labelled. Note the clamp of PsaD connecting the N- and C-terminal domains of this subunit and winding over PsaC. The putative docking site for ferredoxin/flavodoxin is located in the indentation formed by PsaE, PsaC and PsaD.

4.2. Subunit PsaD

Subunit PsaD is involved in the docking of ferredoxin. The direct interaction between these two proteins was shown by chemical crosslinking [30,42], and it has been shown that the crosslinked complex is fully competent in the transfer of electrons from photosystem I to ferredoxin [43]. The position of ferredoxin in these crosslinked complexes was identified by electron microscopy [43]. The same docking site was also found for flavodoxin [44], and is in agreement with a docking site proposed from the structural model of PS I at 6 Å resolution [18]. Subunit PsaD is essential for electron transfer to ferredoxin [45–48]. A solution structure of PsaD could not be determined by NMR [49], possibly because the final folding of this protein is achieved only during assembly into the PS I complex. The main structural motif of PsaD in the PS I complex is a large antiparallel, four-stranded β-sheet followed by a second two-stranded β-sheet. A short loop connects the fourth β-strand to the only α-helix in PsaD. Its main part is buried between PsaC and PsaA, forming ionic interactions with both subunits. A short antiparallel two-stranded β-sheet connects the α-helix to the most remarkable part of PsaD; the amino acids D95 to D123 form a clamp, winding over PsaC (Fig. 3). The large number of interactions between PsaD and the adjacent subunits suggests a stabilising role of PsaD on the stromal ridge and explains why it is needed for correct orientation of subunit PsaC [50,51]. The segment D124–129 forms many hydrogen bonds to PsaB, and the C-terminal region of PsaD is in close contact to the N-terminal region of PsaL in agreement with crosslinking studies [52,53]. This result also explains functional studies, where a destabilisation of PsaD was found in the absence of PsaL [54]. The C-terminus is prominent in this respect, in good

agreement with biotin labelling, proteolysis patterns as well as investigations on mutant photosystem I lacking the 24 residues from the carboxy-terminus of PsaD [48,55].

4.3. Subunit PsaE

Different functions have been reported for PsaE. It is directly involved in the anchoring of ferredoxin [56–58], plays a role in cyclic electron transport [59], and can be crosslinked in barley with the FNR via its N-terminal extension [60]. First evidence for the location of subunit PsaE at the periphery of the stromal hump came from electron microscopy of a mutant lacking the gene of PsaE in cyanobacteria [61]. This was confirmed by the 4 Å structural model of photosystem I [14]. In 1994, the structure of subunit PsaE (8 kDa) in solution was determined by ^{1}H- and ^{15}N-NMR [62]. In solution, subunit PsaE shows a compact structure of a five-stranded antiparallel β-sheets. The loop connecting β-strands 3 and 4 was found to be flexible in the NMR structure. The structure of PsaE in the PS I complex is very similar to the solution structure, with some remarkable deviations in the loop region E-β3β4, which corresponds to the CD loop in the NMR structure. The twist of this loop reported at 4 Å [14] is fully confirmed in the structural model at 2.5 Å resolution [3]. This loop is involved in interactions with PsaA, PsaB and PsaC, suggesting a change of the loop conformation during assembly of the photosystem I complex. The loop E-β2β3 connecting strands E-β2 and E-β3, which points towards the putative docking site of ferredoxin, is close to the loop insertion of PsaC. The fact that PsaE is involved in docking of ferredoxin and flavodoxin [44,63] was questioned by the finding that PsaE deletion mutants are still able to grow photoautotrophically. This contradiction was solved by the discovery that PsaE deletion mutants increased the level of ferredoxin in the cells by orders of magnitude to compensate defects caused by the lack of PsaE [64].

Interactions between PsaE (loop β1/β2) and the C-terminal region of the partially membrane integral subunit PsaF also exist, in good agreement with mutagenesis and crosslinking studies [65]. The interactions of PsaE with PsaC and PsaD are relatively weak, which explains the finding that the geometry of the stromal structure formed by PsaC and PsaD is not dramatically changed in the absence of PsaE [47]. However, the C-terminal region of PsaD, which forms a clamp surrounding PsaC, is in direct contact with PsaE (loop β2/β3), confirming previous crosslinking studies [66].

5. The small, membrane integral subunits

Six small intrinsic membrane protein components of photosystem I have been identified from the gene sequence in *S. elongatus* [17]: the subunits PsaF (15 kDa), PsaI (4.3 kDa), PsaJ (4.4 kDa), PsaK (8.5 kDa), PsaL (16.6 kDa) and PsaM (3.4 kDa). In the 2.5 Å resolution structure [3], a 12th subunit of PS I, PsaX, which contains one transmembrane α-helix, was identified. All of the small membrane integral subunits are located peripherally to the subunits PsaA and PsaB. The main function of the small subunits is the stabilisation of the antenna system and the quaternary structure of photosystem I. The central Mg^{2+} ions of 10 antenna Chl*a* molecules are axially liganded by amino acid side chains or via water molecules by PsaJ, PsaK, PsaL, PsaM and PsaX. Furthermore, subunits PsaF, PsaI, PsaJ, PsaL, PsaM and, to a lesser extent PsaK, are in numerous hydrophobic contacts with the carotenoids. The small subunits can be divided into two groups according to their location in the complex: PsaL, PsaI and PsaM are located in the region where the adjacent monomers face each other in the trimeric PS I complex, whereas PsaF, PsaJ, PsaK and PsaX are located at the detergent exposed surface of photosystem I.

5.1. 'Inside the trimer': PsaL, PsaI and PsaM

PsaL, PsaI and PsaM are located close to the three-fold axis and far away from the lipid exposed surface of the photosystem I trimer [3]. The location of PsaL in the trimerisation domain was first proposed by mutagenesis studies, because no trimers can be detected in PsaL deletion mutants of cyanobacteria [67]. Indeed, PsaL is located close to the C_3 axis in the 'trimerisation domain', forming most of the contacts between the monomers. The N-terminal loop is located on the stromal side harbouring three

small β-strands and one α-helix. A short lumenal loop connects the first and second transmembrane α-helices. Correspondingly the second and third transmembrane α-helices are connected by a short stromal loop. The C-terminus is folded into a short α-helix located in the lumen. The electron density map suggests that a metal ion, possibly a Ca^{2+}, is coordinated by amino acid side chains of PsaL in two adjacent PS I monomers and by PsaA. Possibly, it could be required for stabilisation of the PS I trimer, in agreement with observations in *Synechocystis* sp. *PCC6803* (P. Chitnis, personal communication) that addition of Ca^{2+} stimulates formation of PS I trimers. PsaL coordinates three antenna Chl*a* and forms hydrophobic contacts with carotenoids.

PsaI, which contains one transmembrane helix, is located between PsaL and PsaM, supporting the results of Schluchter et al. [68] who showed that deletion of PsaI influences the stability of these two subunits in the PS I complex in *Synechococcus PCC7002*. Only 10% trimers were found in these mutants, indicating that PsaI stabilises PsaL. A close interaction of PsaL and PsaI was also reported for *Synechocystis PCC6803* [69] and barley [53]. The crystal structure shows that PsaI is in contact with PsaL and also with PsaM, as suggested by Schluchter et al. [68]. It is involved in a few contacts with the adjacent monomer. This subunit does not bind any Chl*a*, but forms hydrophobic interactions with carotenoid molecules.

The existence of close interactions of PsaI and PsaL in higher plants suggests that the arrangement of these small subunits is a motif which is conserved during evolution. This is remarkable, taking into account the fact that plant PS I is a monomer in contact with LHCI complexes [53,70]. This questions the function of the trimer in cyanobacteria. Mutants of *S. elongatus*, which lack PsaL [71], show normal growth at high light intensity, whereas growth under low light was decreased by a factor of 10 compared to wild type [72]. These results suggest that the trimer is essential for optimal light capturing. In plants, close contact between the external light harvesting complexes LHCI and PsaL was suggested from results of crosslinking studies [53], supporting the idea that the function of PsaL is to facilitate the 'input' of excitation energy from the external antenna complexes in plants. This would correspond to excitation energy transfer between the monomers in the trimeric PS I from cyanobacteria, in agreement with results and suggestions of Karapetyan et al. [73].

PsaM (3.4 kDa) is the smallest subunit of photosystem I and has been predicted to contain only one transmembrane α-helix [17]. This subunit has only been found in cyanobacterial photosystem I. Although an open reading frame for this subunit was also found in liverwort chloroplast genome [74], this subunit was not identified thus far in any preparation of plant photosystem I. Deletion of subunit PsaM in cyanobacteria seems to have an indirect effect on the stability of the system and the electron transport reactions [68]. Different locations of PsaM have been suggested in the previous X-ray structural models at medium resolution, whereas PsaM is identified unambiguously in the 2.5 Å structure. It is located close to the monomer/monomer interface, in the neighbourhood of PsaI and PsaB (see Fig. 1a and b). In agreement with the structure predictions from hydrophobicity plots [17], it contains only one transmembrane α-helix. The N-terminus is located in the lumen, the C-terminus in the stroma. PsaM forms hydrophobic contacts with a carotenoid molecule and is involved in the coordination of one Chl*a*.

5.2. 'Distal side': PsaF, PsaJ, PsaX and PsaK

For a long time, it was expected that subunit PsaF was an extrinsic subunit located at the lumenal side of photosystem I. This assumption was mainly based on the fact that subunit PsaF in plants contains two pre-sequences: one for the import into the chloroplast and a second for import into the thylakoid lumen. Recently it was shown that this protein is imported by the same pathway as that used for the import of plastocyanin (the soluble lumenal electron carrier) [75–77]. First evidence for an – at least partial – membrane intrinsic location of subunit PsaF came from the finding that subunit PsaF cannot be extracted with chaotropic agents (e.g. urea or NaBr) [78], but can be removed by detergents such as Triton X-100 [79]. Hydrophobicity plots show one or two sequence regions which could span the membrane [80]. Further evidence for at least one membrane span in subunit PsaF was provided by results of experiments [54] where subunit PsaF could be

crosslinked with the stromal subunit PsaE. These observations can be only explained if subunit PsaF spans the membrane at least once. As discussed previously, PsaF is involved in the docking of plastocyanin in plants [81–84], but not in cyanobacteria [26]. The structure of subunit PsaF consists of two domains. In agreement with biochemical studies [85], the N-terminal domain is located at the lumenal side of the complex, with α-helices F-c and F-d being the most prominent features. These hydrophilic α-helices are parallel to the membrane plane and are located at ≈15 Å distance to the putative docking site of cytochrome c_6. Although PsaF is not directly involved in electron transfer from cytochrome c_6 to P700 in cyanobacteria, this part of PsaF could play an important role in the stabilisation of the lumenal surface of photosystem I. The C-terminal domain of PsaF is mainly membrane intrinsic. PsaF contains only one transmembrane α-helix F-f, followed by two shorter hydrophobic α-helices F-g and F-h. α-Helix F-h enters the membrane from the stromal side and ends in the first third of the membrane. It is followed after a crease by α-helix F-i, running back to the stromal side, where the C-terminus is located and forms contacts with PsaE in agreement with crosslinking studies [54]. In contrast to previous suggestions [12,15], PsaF does not axially coordinate chlorophylls, but forms hydrophobic interactions with several carotenoids. A possible role of the transmembrane part of PsaF could be a shielding of the carotenoids and chlorophylls from the lipid phase. A possible further function of PsaF in cyanobacteria could be an interaction with the external antenna system of phycobillisomes. This is supported by the observation that deletion of PsaF in *S. elongatus* leads to a growth defect at low light intensity, accompanied by a dramatic increase of allophycocyanin, giving the whole cell suspension a turquoise colour (P. Jordan and P. Fromme, unpublished). In plants, a direct contact of PsaF with the plant light harvesting systems has been suggested by experiments in which plant subunit PsaF was isolated as a Chl–protein complex with LHCI proteins [86].

A location of PsaJ close to PsaF was predicted by mutagenesis and crosslinking experiments on the cyanobacterial [26,87] and plant photosystem I [53,85]. The N-terminus of PsaJ is located in the stroma, the C-terminus is located in the lumen. PsaJ contains one transmembrane α-helix. It binds three chlorophylls and is in hydrophobic contact with carotenoids.

A single transmembrane helix in neighbourhood to PsaF, which was tentatively assigned to PsaJ at 4 Å resolution [15], was identified as a 12th subunit of PS I at 2.5 Å resolution. A small polypeptide was identified in dissolved crystals of PS I, which revealed a short N-terminal sequence (W. Schröder, in preparation) homologous to that of the controversial subunit PsaX, so far only identified by N-terminal sequencing in PS I from the thermophilic cyanobacteria *Synechococcus vulcanus* and *Anabaena variabilis* [88,89]. The electron density map at 2.5 Å resolution was well defined so that large side chains could be predicted and shown to be consistent with the amino acid sequences of PsaX known from N-terminal sequencing. The structural model of PsaX contains 29 residues. The six stromally located N-terminal amino acids were not identified in the structure, possibly because this part of the structure is flexible. It is remarkable that no gene sequence for PsaX has yet been published so far and yet a homologous gene is not found in the mesophilic cyanobacterium *Synechocystis PCC6803* where the genome is completely known. The question whether PsaX is a unique subunit of thermophilic cyanobacteria, necessary for stability of the PS I complex at higher temperatures, has to be solved by sequencing of genomes of different thermophilic and mesophilic cyanobacteria.

In the electron density map at 2.5 Å resolution, subunit PsaK, which contains two transmembrane α-helices as predicted from the sequence [17], was found to be located at the periphery of the PS I complex. These two α-helices were not detected at 4 Å resolution [14]. At 2.5 Å resolution, PsaK appears to be the least ordered subunit in the PS I complex, as indicated by high temperature factors, so that an unambiguous sequence assignment was not possible and the structure was modelled with polyalanine. Although the polypeptide backbone of PsaK as modelled into the electron density map is not continuous, the loop connecting both α-helices is most likely located in the stroma. The proposed location of this loop is in agreement with the 'positive inside rule' described in [90], which was based on the finding that strongly positively charged loops connecting transmembrane α-helices can not be translocated through the membrane during insertion and

assembly of membrane proteins. In agreement with crosslinking studies [53], PsaK is not in contact to any other of the small membrane intrinsic proteins. PsaA is the only subunit in immediate neighbourhood of PsaK. The protein coordinates two chlorophylls and forms contacts with carotenoids. PsaG, a subunit unique to plants, shows sequence similarity to PsaK, leading to the suggestion that these proteins have the same genetic origin [91]. It can be speculated [53], that PsaG in plants could be located at the opposite site of the PS I complex close to PsaB, at a position related to PsaK by the local pseudo-C_2 symmetry axis.

6. The electron transfer chain

The electron transfer chain, which mediates the transmembrane charge separation, is the functionally most important part of photosystem I. The kinetics and energetics of electron transfer were investigated by spectroscopy during the last few decades (for review see [7]). The electron transfer carriers as identified by spectroscopy are as follows: P700, the primary donor (probably a dimer of Chl*a* molecules) where charge separation is initiated, A_0 (a Chl*a* molecule), A_1 (a phylloquinone), and the three [4Fe4S] clusters F_X, F_A and F_B.

The general arrangement of the chlorophyll and quinone cofactors of the electron transfer chain was shown to be similar in photosystem I and in type II reaction centres at medium resolution [10,12,13,15], leading to the suggestion that all photosynthetic reaction centres evolved from a common ancestor [8,10,92]. Despite this similar structural arrangement of cofactors, large differences in the physico-chemical properties of corresponding cofactors and in the kinetics of the electron transfer have been observed (for review see [7,93]).

The structure at 2.5 Å resolution shows, for the first time, the structural details of the cofactors and the protein–cofactor interactions, which define the energetics and kinetics of electron transfer. Six chlorophyll molecules, two phylloquinones and three [4Fe4S] clusters, of which the organic cofactors are arranged in two branches as pairs of molecules related by the pseudo-C_2 axis, constitute the ETC (Fig. 4). The pairs of chlorophylls of the ETC are labelled eC followed by A or B indicating whether PsaA or PsaB is involved in the axial coordination of the Mg^{2+} ion, and by numbering from 1 to 3 starting from the lumenal side. It is remarkable that the cofactors forming one branch are not bound exclusively to one subunit of PS I. The A-branch features the chlorophylls eC-A1, eC-B2, eC-A3 and the phylloquinone molecule Q_K-A, the B-branch the chlorophylls eC-B1, eC-A2, eC-B3 and the phylloquinone Q_K-B.

The manner in which photosystem I functions will be discussed in the following by combining information about the energetics and kinetics of electron transport with information about structural features of the individual electron carriers, the role of the protein in the coordination of cofactors and a possible direct influence on the electronic structure of the cofactors by the protein environment.

6.1. The primary electron donor P700

After P700 is excited to its lowest excited state, P700*, an electron is very rapidly (within 1–3 ps) transferred to A_0 [94]. P700* has a highly negative redox potential (about −1300 mV), and is hence a very strong reductant. The reaction free energy ΔG_0 for the initial charge separation step was estimated to be 250 meV (see [7] for a detailed discussion of the energetics and kinetics of the electron transfer chain).

Years of discussion and a great deal of effort was put into studies to answer the question of whether P700 exists as a dimer or a monomer of Chl*a* (for a review, see [95]). Investigations on the triplet state of P700 indicate that ^{3}P700 has a dimeric nature [96,97]. The cation $P700^{+\bullet}$ was investigated by magnetic resonance and infrared spectroscopic techniques [98,99]. The results clearly show that the spin density of $P700^{+\bullet}$ is unequally distributed between the two chlorophylls that constitute $P700^{+\bullet}$. About 85% of the spin density is located on one of the two chlorophylls. Electron nuclear double resonance (ENDOR) on single crystals [100,101] shows that this chlorophyll is oriented perpendicular to the membrane plane. A dimeric structure of P700 was proposed from the X-ray structural models of PS I at 6 Å and 4 Å resolution [11,12], however ring substituents and asymmetric features of the ring system of the chlorophylls were not visible, so that information

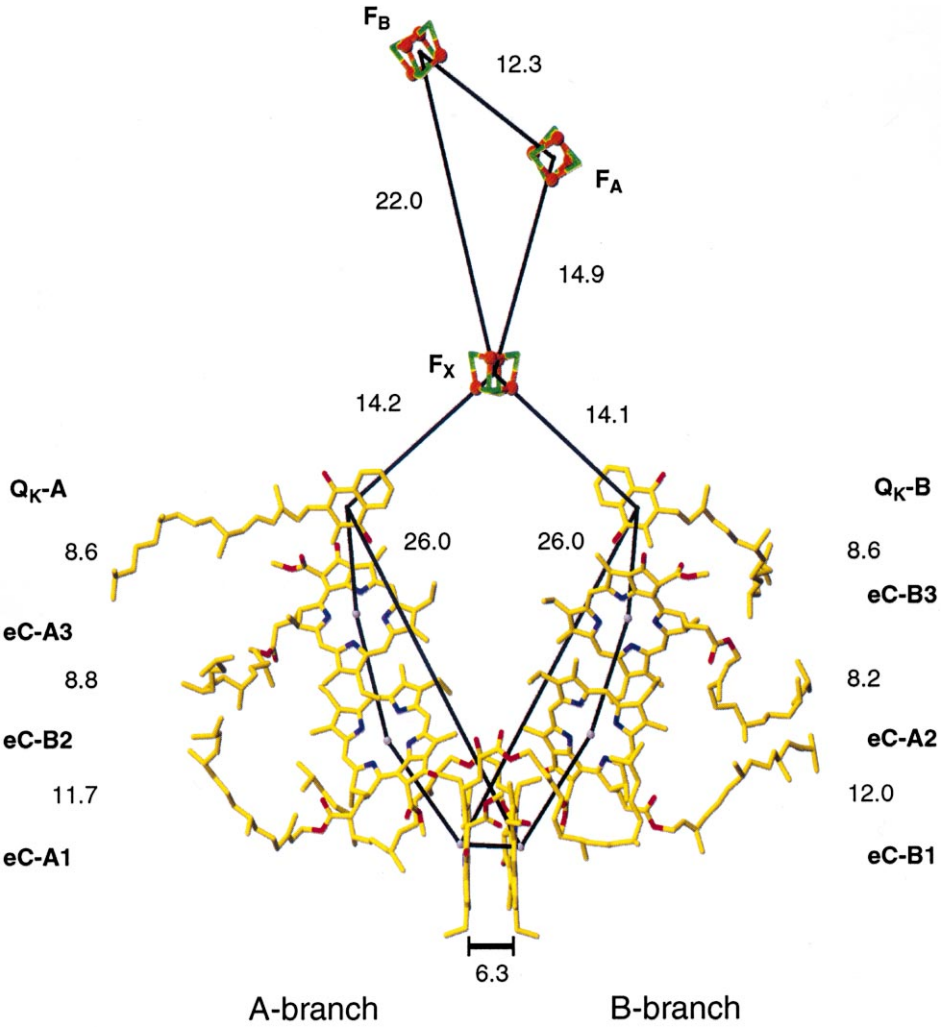

Fig. 4. The electron transfer system of PS I. View direction perpendicular to the membrane normal. The organic cofactors (yellow) on the left-hand side belong to the A-branch, those on the right-hand side to the B-branch. The three [4Fe4S] clusters F_X, F_A and F_B are located stromal of these cofactors. At the left and right margins the names of the cofactors are given. Centre to centre distances (in Å) between the corresponding cofactors are indicated.

about the direction of the Q_X and Q_Y transition dipoles and about the protein environment was lacking. However, it was suggested that the single histidine in the transmembrane α-helices, which correspond to the hydrophobic stretches X of PsaA and PsaB (corresponding to helices A/B-j in the 2.5 Å structure), could provide the fifth ligands to the Mg^{2+} ions of the two chlorophylls of P700 [12,13,15,18]. This suggestion was further supported by results of EPR investigations [102]. Furthermore, studies indicate that the spin carrying chlorophyll is coordinated by this histidine in PsaB [103–105].

Models of P700, in which P700 and the 'special pair' of the RC of purple bacteria are in a similar arrangement, have been suggested from spectroscopic results [96].

In the crystal structure, the primary donor P700 is represented by the chlorophyll pair eC-A1 and eC-B1, located at the lumenal side of the membrane (see Fig. 5). The distance between the Mg^{2+} ions of these two chlorophylls is 6.3 Å, which is shorter than the corresponding distance between the bacteriochlorophylls in the special pair of PbRC. The planes of eC-A1 and eC-B1 are oriented perpendicular to the membrane plane and parallel to each other with an

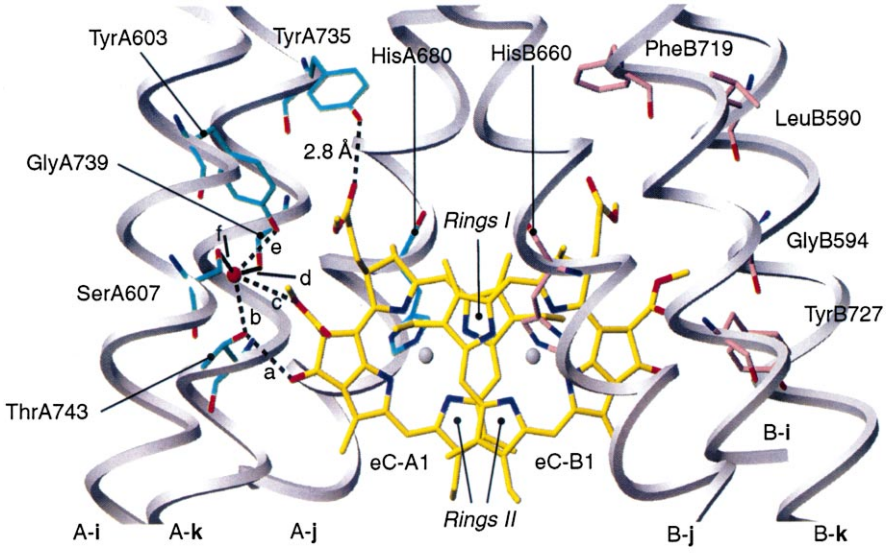

Fig. 5. The primary donor P700 and its protein environment. View direction parallel to the membrane plane perpendicular to the chlorin planes of the chlorophylls. The longest part of the phytyl side chains of the two chlorophylls has been omitted for clarity. The helices surrounding the two chlorophylls eC-A1 and eC-B1 are shown as grey ribbons. Residues of PsaA involved in hydrogen bonds (dashed black lines) to the water molecule (red sphere) or eC-A1 are coloured green. The corresponding amino acid residues of PsaB are coloured pink. All six theoretically possible hydrogen bonds in the vicinity of ring V of eC-A1 are labelled with letters a to f, with the details given at the bottom of the figure.

interplanar distance of 3.6 Å. The overlap between the ring systems differs between P700 in photosystem I and the special pair of PbRC. In the bacteriochlorophyll ring system in the special pair, the rings I overlap perfectly [21], whereas the rings I and II of the chlorophylls only partially overlap in P700 (see Fig. 5). This implies a weaker electronic interaction between the π electron systems in P700 than in the special pair of PbRC. While the latter consists of a homodimer of BChl molecules, the electron density map clearly reveals that P700 does not consist of two Chl*a* molecules, but is a heterodimer consisting of a Chl*a* molecule and a Chl*a*′ molecule, the C13^2-epimer of Chl*a*. This finding now confirms previous results of Watanabe et al., Maeda et al. and Maroc and Tremolieres [106–108], who suggested that P700 contains one or two Chl*a*′ molecules on the basis of chlorophyll extraction experiments. The Chl*a*, eC-B1, is located in the B-branch and is axially coordinated to HisB660, whereas the Chl*a*′, eC-A1, which is located in the A-branch, is axially coordinated by HisA680. The asymmetry of P700 proceeds to differences in the chlorophyll binding pockets for eC-A1 and eC-B1. In the A-branch, the Chl*a*′ molecule, C-A1, forms hydrogen bonds to side chains of transmembrane α-helices A-i and A-k and a water molecule (Fig. 5). However, no hydrogen bonds to the Chl*a* molecule, eC-B1, are established in the B-branch. Differences in hydrogen bonding influence the spin density distribution, as shown for the special pair in PbRC by Artz et al. [109]. The translation of their results to the situation in photosystem I leads us to suggests that the electron spin density in $P700^{+\bullet}$ may be localised to a larger extent on the non-hydrogen bonded Chl*a* half (eC-B1) of the P700 dimer. This would agree with results from ENDOR and mutagenesis studies, showing that PsaB is probably the subunit, which binds the chlorophyll carrying more than 80% of the electron spin density in $P700^{+\bullet}$ [99,101].

6.2. *Second and third pairs of chlorophylls of the electron transport chain*

The initial charge separated state $P700^{+\bullet}/A_0^{-\bullet}$ is very difficult to investigate spectroscopically in intact photosystem I for two reasons: (i) $A_0^{-\bullet}$ is short-lived and reaches only a low maximal concentration. The half life times needed for excitation energy transfer (20–30 ps) from the antenna system to P700 and reoxidation of $A_0^{-\bullet}$ (20–50 ps) are comparable, longer than the time required for initial charge separation (1–3 ps) [110–113]. (ii) All phorphyrins in photosystem I are Chl*a* type molecules, therefore $A_0^{-\bullet}$ can hardly be detected in intact photosystem I. However, optical difference spectra of partly Chl depleted PS I indicate that A_0 can be represented by a monomeric Chl*a* molecule [114].

In the X-ray structural models of photosystem I at medium [12] and high resolution [3], three pairs of chlorophylls are present in the electron transport chain. The chlorophylls of the second pair (namely eC-B2 and eC-A2) have a centre to centre distance of $\approx$12 Å to the chlorophylls of P700. These two chlorophylls are the only cofactors of the ETC where the coordinating subunit of the A-branch is PsaB and vice versa. In both branches, a water molecule pro-

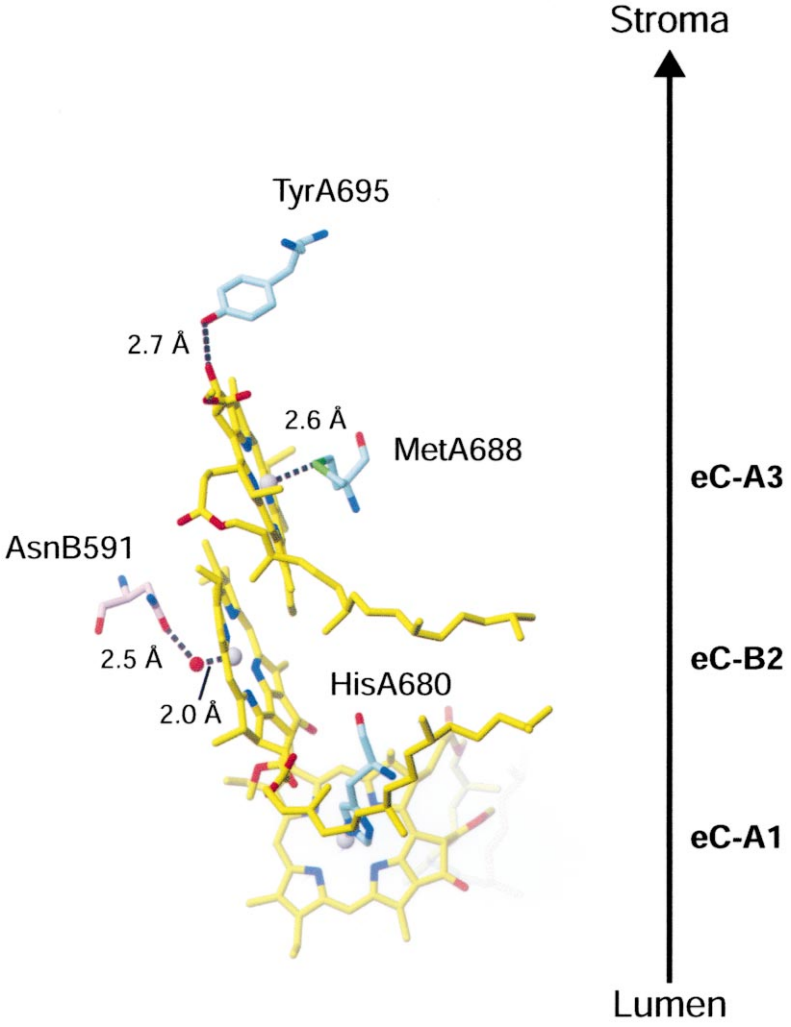

Fig. 6. The chlorophyll cofactors eC-A1, eC-B2 and eC-A3 of the A-branch of the ETC. View direction is parallel to the membrane plane. Non-hydrophobic interactions of eC-B2 and eC-A3 with neighbouring side chains of PsaA and PsaB are indicated by dashed black lines. The axial ligand of the central Mg^{2+} ion of eC-B2 is a water molecule (red sphere) which is hydrogen bonded by AsnB591. eC-A3 is axially liganded by MetA688 and forms an additional hydrogen bond with TyrA696.

vides the fifth ligand to the central Mg^{2+} ion of the second pair of chlorophylls. The water molecule which provides the axially ligand to the Chl*a* at the A-branch, is hydrogen bonded to asparagine residue AsnB591 (see Fig. 6); thus this chlorophyll molecule is named eC-B2. The binding pocket of the corresponding chlorophyll in the B-branch is similar, so that AsnA604 is hydrogen bonded to the water molecule, which axially ligands the chlorophyll eC-A2 (data not shown). Neither chlorophyll forms any hydrogen bonds. Remarkable differences are observed in the orientation and coordination of the second pair of chlorophylls/bacteriochlorophylls ('accessory (bacterio)chlorophylls') between photosystem I and the PbRC, in which histidines provide the fifth ligand for the Mg^{2+} [21,115].

The structure of photosystem I at 2.5 Å resolution strongly supports the idea that the chlorophylls eC-A2 and eC-B2 may be directly involved in electron transfer from P700 to A_0. In this respect it should be noted that these chlorophylls are located close ($\approx$3.8 Å) to the next chlorophylls of the ETC, eC-A3 and eC-B3, with a roughly parallel orientation of the chlorine rings of eC-B2⟨=⟩eC-A3 and eC-A2⟨=⟩eC-B3. Taking this close proximity into account, it seems to be reasonable that the spectroscopic and redox properties of eC-A3 and eC-B3 may be influenced by eC-B2 and eC-A2, respectively. This suggestion is supported by the finding that the difference spectrum $A_0/A_0^{-\bullet}$ contains contributions from more than one chlorophyll [116].

The third pair of chlorophylls (Chl*a* eC-A3 and Chl*a* eC-B3) is located in the middle of the membrane. It can be assumed that one or both of them represent the spectroscopically identified electron acceptor A_0. The axial ligands of these two chlorophylls are very unusual: the fifth 'ligands' of the Mg^{2+} ions are provided by the sulfur atoms of methionine residues A688 and B668 (d_{Mg-S} = 2.6 Å), respectively (Fig. 6). This structural result is remarkable, because the concept of hard and soft acids and bases predicts only weak interactions between the hard acid Mg^{2+} and methionine sulfur as a soft base. The structure shows that each of the two chlorophylls eC-A3 and eC-B3 constitute one hydrogen bond between the hydroxyl groups of tyrosines A696 and B676 (d_{O-O} = 2.7 Å) and the keto oxygens of rings V of eC-A3 and eC-B3, respectively. The question whether the very low redox potential of the electron acceptor A_0 (~ -1050 mV) is caused by lack of a strong fifth ligand to the Mg^{2+} atom of these chlorophylls remains to be answered.

A sequence comparison between photosystem I complexes from cyanobacteria, green algae and higher plants reveals that all amino acids which are involved in axial coordination and hydrogen bonding to the second and third Chl*a* pairs of the ETC are strictly conserved. The conservation of the differences in the axial coordination and hydrogen bonding between the three pairs of chlorophyll molecules throughout evolution could suggest that these protein–chlorophyll interactions are essential for the physico-chemical properties (e.g. the redox potentials) of these cofactors. The participation of each of these chlorophyll molecules in electron transfer can be assumed, because the edge to edge distances between adjacent chlorophylls of the ETC are very short ($\approx$4 Å). However direct experimental evidence for the involvement of the 'accessory chlorophylls' in forward electron transfer as it is found in purple bacterial reaction centres [117], is lacking for photosystem I for the reasons mentioned above.

6.3. The secondary electron acceptor A_1/vitamin K1

The electron transfer from $A_0^{-\bullet}$ to A_1, a phylloquinone, occurs within 20–50 ps [110]. The free energy gap for this step was estimated to be in the order of ΔG_0 = 340 meV [118]. In the same publication it was estimated that the reorganisation energy λ is of the same order of magnitude as the free energy gap, i.e. $-\Delta G_0 \approx \lambda$, which is the optimal condition to get rapid electron transfer [119].

There are two phylloquinone molecules present in photosystem I. They are both tightly bound, in contrast to those in PbRC and PS II, where the quinone Q_A is tightly bound and Q_B is mobile, leaving the binding pocket after double reduction and uptake of two protons. In PS I, the phylloquinone is singly reduced and involved in ET to the first iron sulfur centre F_X. Both quinones were extracted by organic solvents, one of them being more easily removed than the other [120,121]. The electron transfer to F_X was not affected by the extraction of the first quinone, but was blocked following the extraction of the second. These results may be interpreted to

provide an argument for the suggestion that only one of the quinones is actively involved in electron transfer. However, this result could be also obtained if both quinones are normally active, but electron transfer is all routed via the residual quinone when the first quinone is removed. Furthermore, these data were not fully reproduced later [122], so that the question of whether only one or both branches are active in electron transfer is still open and will be discussed below.

The structure of PS I at 2.5 Å resolution shows two phylloquinones, Q_K-A and Q_K-B, at centre to centre distances of 8.6 Å to eC-A3 and eC-B3, respectively, within the same branch. Their position is consistent with photovoltage measurements indicating that the transmembrane distance between A_0 and A_1 is only about 20% of the corresponding distance from P700 and A_1 [111], compared to $\approx$30% as determined in the crystal structure. The axis connecting the two oxygens points towards P700 in good agreement with suggestions based on EPR experiments [123,124]. The distance between $P700^{+\bullet}$ and $A_1^{-\bullet}$ was determined by pulsed EPR measurements to be 25.4 ± 0.3 Å [125,126]. This result is in agreement with the centre to centre distances of 26.0 ± 0.3 Å, derived from the 2.5 Å structure for the cofactors of the pairs eC-A1/Q_K-B and eC-B1/Q_K-A. The centre to centre distances between pairs of P700 chlorophylls and quinones in the same branch, eC-A1/Q_K-A and eC-B1/Q_K-B, are 24.2 ± 0.3 Å and 24.4 ± 0.3 Å; too short to be in agreement with the distance determined by EPR.

The question regarding the nature of the binding pocket can now be addressed. The phylloquinone binding sites in PS I for Q_K-A and Q_K-B are nearly identical but do differ from the Q_A binding site in PbRC. Two conserved tryptophans, TrpA697 and TrpB677, located on the stromal surface α-helices A/B-jk(1), respectively, form the most prominent interactions with the phylloquinones. The interplanar distances between the aromatic ring systems of the tryptophans TrpA697 and TrpB677 and the quinones Q_K-A and Q_K-B, respectively, range from 3.0 Å to 3.5 Å, indicating strong interactions between the π electron systems (π stacking). These results are in agreement with structural modelling studies based on EPR data and the medium resolution X-ray structure [13,127] as well as ideas based on results of quinone reconstitution experiments [128]. In both phylloquinones Q_K-A and Q_K-B, only one of the two carbonyl oxygen atoms is hydrogen bonded. This is in contrast to the EPR results, which indicate that there are two hydrogen bonds to $A_1^{-\bullet}$ [129]. The reason for this discrepancy is unclear, but small con-

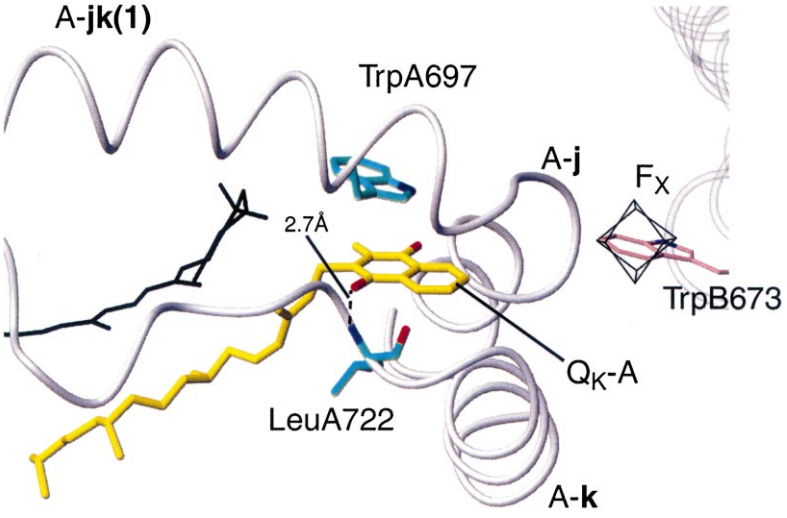

Fig. 7. The environment of the phylloquinone Q_K-A. View direction from the stromal side onto the membrane plane into the phylloquinone binding site at the A-branch of the ETS. The phylloquinone Q_K-A is depicted in yellow. The grey ribbon represents the main chain of PsaA, the residues of which form the binding pocket of Q_K-A. LeuA722 and TrpA697, interacting with the quinone, are explicitly shown in green. On the left-hand side a carotenoid located near the quinone is drawn in black. On the right-hand side the [4Fe4S] cluster F_X is shown. Lumenal of the cluster TrpB673 is located.

formational changes in the quinone binding sites during reduction can not be excluded. The carbonyl oxygen at the ortho position to the phytyl chains of Q_K-A and Q_K-B accepts hydrogen bonds from backbone NH groups of LeuA722 and LeuB706, respectively (for details see Fig. 7). The lack of a second hydrogen bond is remarkable, because in all other enzymes of known structure that contain tightly bound quinones, hydrogen bonding to both carbonyl oxygens is observed [21,115,130–134]. The asymmetric hydrogen bonding could contribute to the lower redox potential (~ -820 mV) [128] of the phylloquinone in PS I with respect to Q_A (~ -130 mV) in PbRC and PS II.

The question of whether one or two branches are active in electron transfer is most controversially discussed in the literature (for review see [1]). The primary donor P700 is the only site, at which a significant difference between the two branches is obvious from the structure at 2.5 Å resolution. As previously discussed, the spin density in $P700^{+\bullet}$ is presumably located on the Chl*a* eC-B1. The cofactor pair eC-$B1^{+\bullet}$/Q_K-$A^{-\bullet}$, at a centre to centre distance of 26.0 Å, is in agreement with the distance between $P700^{+\bullet}$ and $A_1^{-\bullet}$ determined by EPR spectroscopy at 4 K [125]. Thus it is concluded that the phylloquinone identified by EPR spectroscopy is Q_K-A, in agreement with mutagenesis studies [135]. Kinetic investigations proposed that the electron transfer between A_1 and F_X, with $t_{1/2}$ of 200 ns corresponding to a rate of $3.4 \cdot 10^6$ s^{-1}, is the rate limiting step for the whole electron transfer in PS I. From the edge to edge distance between Q_K-A and the cysteine ligands of F_X ($R = 6.8$ Å) a maximal rate of $k_{ET}|-\Delta G_0 = \lambda| = 8.3 \cdot 10^{10}$ s^{-1} can be calculated using the empirical equation $\log k_{ET} = 15 - 0.6R - 3.1(\Delta G_0 + \lambda)^2/\lambda$ [119], where ΔG_0 is the reaction free energy and λ the reorganisation energy. The free energy gap for the electron transfer step from A_1 to F_X was calculated to be -54 meV [136]. It is evident from the discrepancy between the observed rate and the calculated maximal rate that $-\Delta G_0 \neq \lambda$, leading to the conclusion that a significant activation energy, ΔG^*, exists. A value of $\Delta G^* = 220 \pm 20$ meV was determined from the temperature dependence of k_{ET} leading to an estimation of $k_{ET}|-\Delta G_0 = \lambda| = 9 \cdot 10^{10}$ s^{-1} [137] which is in good agreement with the rate of $8.3 \cdot 10^{10}$ s^{-1} calculated on the basis of the crystal structure. Summarising the points discussed above, it can be stated that the conclusions drawn by Schlodder et al. [137] are supported by the recent structural results [3]. The phylloquinone, detected by EPR spectroscopy, is Q_K-A and the electron transfer from this phylloquinone to F_X is slow because a significant activation energy barrier exists. Nevertheless, the results do not exclude an electron transfer along the B-branch, which is so fast that Q_K-B can not be detected on the time scale of EPR spectroscopy. Recently, strong evidence based on mutagenesis studies of the tryptophans in both quinone binding sites in PS I [138,139] was achieved in favour of the proposal that both branches are active in forward electron transfer. The A-branch was proposed to be the slower, with $t_{1/2} = 200$ ns, whereas the electron transfer from the quinone to F_X occurs with $t_{1/2} = 15$–25 ns in the B-branch. The structure shows that the distances from Q_K-B and Q_K-A to F_X are identical, leading to the conclusion that ΔG^* must be lower in the B-branch than in the A-branch. The binding pockets of the phylloquinones in PsaA and PsaB show no obvious differences, however long range interactions and small changes in the coordination sphere could also contribute to this reduction. The most remarkable differences between PsaA and PsaB in this region are the tryptophan TrpB673, which is not conserved in PsaA and located between Q_K-B and F_X, and the different chemical natures of the lipids (I) and (II) located at positions which are related by the pseudo-C_2 axis. Phospholipid (I) is located at a distance of 15 Å to Q_K-A and the galactolipid (II) at a distance of 15 Å to Q_K-B. Site directed mutants in the vicinity of these cofactors must be constructed to illuminate this further.

6.4. The first FeS cluster, F_X

The iron sulfur clusters are the terminal electron acceptors of type I reaction centres. The first [4Fe4S] cluster, F_X, plays a prominent structural role in addition to its essential role in electron transfer. The pseudo-C_2 axis, relating the two large subunits PsaA and PsaB to each other, runs through the centre of the iron sulfur cluster F_X (Fig. 8). It was already proposed from the amino acid sequences that the iron sulfur centre F_X is coordinated by four cysteines, two from each of the subunits PsaA and

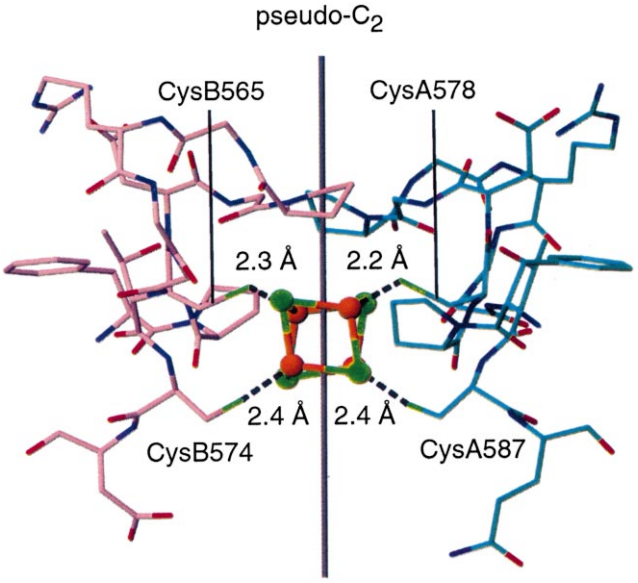

Fig. 8. The [4Fe4S] cluster F_X and its protein environment. The view direction is parallel to the membrane plane. Sulphur atoms shown in turquoise, iron atoms in orange, carbon atoms of PsaA in green and of PsaB in pink. Coordination of the Fe atoms by the conserved cysteine residues indicated by dashed lines, distances in Å.

PsaB [16,17]. This binding motif is located between the transmembrane α-helices VIII and IX, the α-helices A/B-i and A/B-j in the structure at 2.5 Å resolution [3]. The location of the first [4Fe4S] cluster, F_X, is defined by a pocket of high electron density and the cysteine ligands to the iron ions. As shown by mutagenesis studies [140,141] and kinetic investigations [142–144], F_X plays an important role in the assembly and the structural integrity of photosystem I as well as in electron transfer.

The kinetics of electron transfer from F_X to the terminal iron sulfur clusters of PS I, F_A and F_B, are faster than the electron transfer from A_1 to F_X. The kinetics are difficult to determine because the optical difference spectra of the three [4Fe4S] clusters are nearly identical [145]. The fast electron transfer explains why F_X is not detected in EPR spectra in intact PS I complexes at moderate conditions because the level of $F_X^{-\bullet}$ is low. Nevertheless, F_X can be detected during strong illumination under conditions where F_A and F_B had been chemically prereduced [1]. From F_X the electron is transferred via F_A to the terminal iron sulfur cluster F_B. Both clusters are bound to PsaC and have been discussed above. The electron reaches the soluble electron carrier ferredoxin in 500 ns [146], which leaves the docking site after reduction and transfers the electron to the FNR for reduction of $NADP^+$.

7. The structural organisation of the core antenna system

Photosystem I contains an integral antenna system consisting of about 90 Chl*a* molecules and 22 carotenoids. It shows no structural similarity to the highly symmetric bacteriochlorophyll arrangements in the light harvesting complexes of purple bacteria [147,148]. The chlorophylls have dual functions in PS I: six of them are constituents of the electron transport chain and have been discussed above. The remaining 90 chlorophylls are used to capture light and belong to the antenna system of PS I.

The role of the carotenoids in photosynthesis is more complex. There are at least five different functions of carotenoids: light harvesting, photoprotection, protection against singlet oxygen, excess energy dissipation and structure stabilisation (for a review, see [149]).

The time taken for the energy transfer from the antenna system to P700, the 'trapping time', depends on the organism and the antenna size [150–153]. Values between 20 and 35 ps have been reported. There is strong evidence that after excitation, the energy is rapidly distributed between the chlorophylls in the antenna system in an equilibrium process (with 3.7–7.5 ps lifetime) [116]. This happens before trapping occurs [154]. The excitation energy transfer and trap-

→

Fig. 9. All cofactors of photosystem I, with special regard to the antenna system. (a) View from the stromal side onto the membrane plane. (b) Side view of the cofactors of PS I, the view direction is parallel to the membrane plane. Organic cofactors of the ETC are coloured blue. The [4Fe4S] clusters are coloured orange and yellow. The dashed lines underline the organisation of the PsaA/PsaB bound antenna chlorophylls (yellow) in one central and two peripheral domains. The chlorophylls bound to the peripheral subunits and the phospholipid are coloured grey. The chlorophylls referred to as 'red chlorophylls' are shown in red. The carotenoids are organised in six clusters which are marked by black ellipsoids.

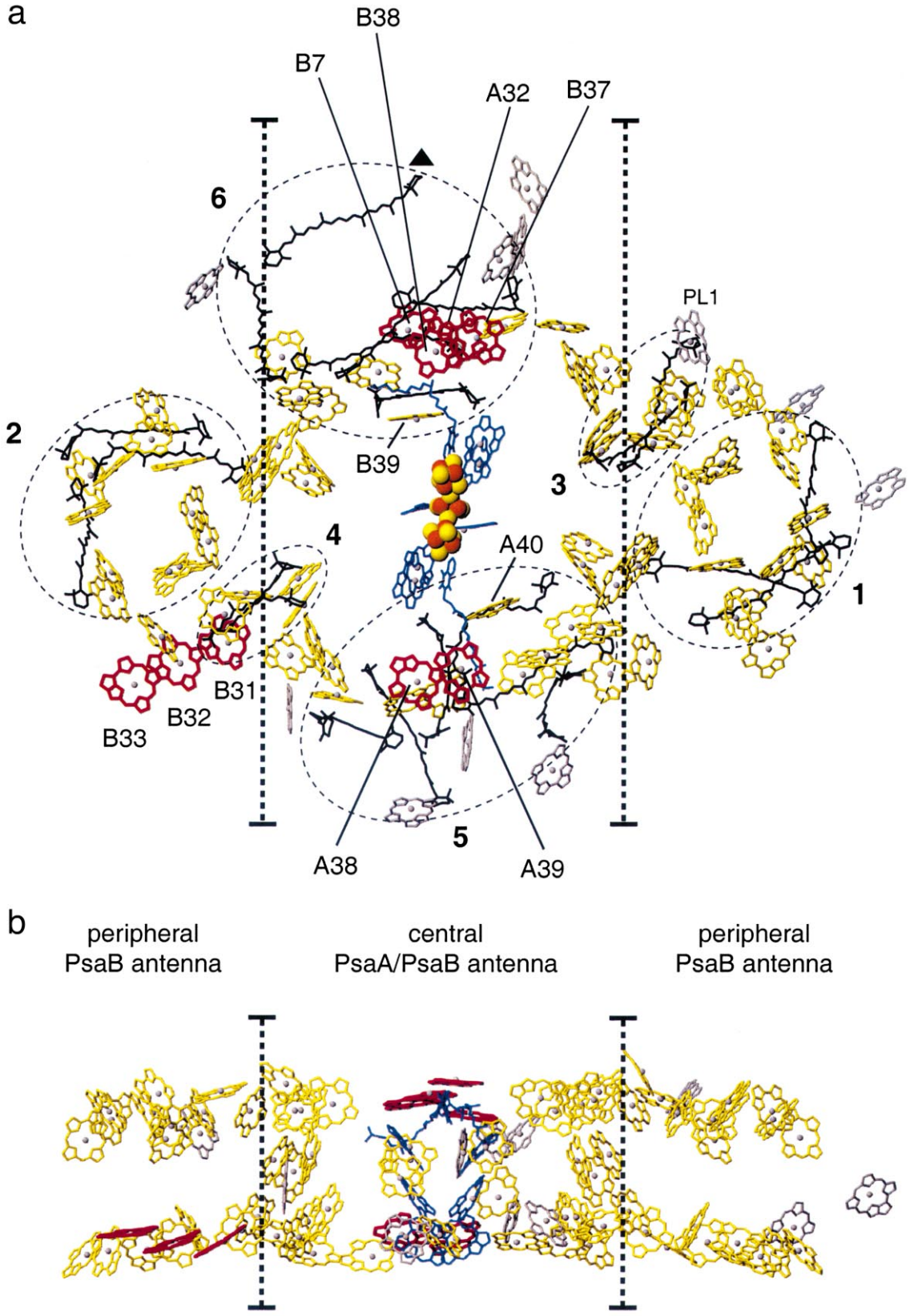
a
B38
B7
A32
B37
6
PL1
2
B39
3
4
A40
1
B31
B32
B33
5
A38
A39
b
peripheral
PsaB antenna
central
PsaA/PsaB antenna
peripheral
PsaB antenna

ping in photosystem I was described as a transfer to the trap limited process [155].

7.1. The antenna chlorophylls

The large subunits PsaA and PsaB bind 79 of the 90 antenna chlorophylls (see Table 1). Furthermore, 10 Chl*a* molecules are axially liganded by the small membrane intrinsic proteins PsaJ, PsaK, PsaL, PsaM and PsaX. The Mg^{2+} ions of the chlorophylls are axially coordinated either directly by atoms of amino acid side chains (imidazole moieties of His, oxygen atoms of Gln, Asp, Glu or the hydroxyl group of Tyr), by peptide carbonyl oxygens or indirectly via water molecules. Interestingly, a phosphatidylglycerole (PG) also provides the fifth ligand of the Mg^{2+} ion of a Chl*a* molecule (PL1 in Fig. 9a). Together with those effects discussed below for the 'red' chlorophylls, these differences in axial coordination of the central Mg^{2+} ions may contribute to the observed wide absorption range of the chlorophylls in PS I.

Those chlorophylls of the antenna system which are bound to PsaA and PsaB can be divided into three distinct domains: the central domain, surrounding the inner α-helices, where the chlorophylls are distributed over all depths of the membrane, and two peripheral domains, where the chlorophylls form layers on the stromal and lumenal sides of the membrane (Fig. 9b). At medium resolution [12,15], $\approx$10 Chl*a* which are located in these layers were not identified; therefore this layer structure was only partially visible.

The chlorophylls bound to PsaA and PsaB loosely follow the pseudo-C_2 symmetry. For the majority of the antenna chlorophylls, the centre to centre distances to their nearest neighbour Chl*a* are in the range from 7 to 16 Å. This is a range, in which Förster type fast excitation energy transfer is favourable [156].

The electron transport chain and the antenna system are well separated, but there are two chlorophyll molecules, aC-A40 and aC-B39, which seem to connect the antenna system structurally to the electron transfer chain. They are in close proximity to the two chlorophyll molecules of the ETC, aC-A40 at a centre to centre distance of 12.8 Å to eC-A3 and aC-B39 at 10.9 Å to eC-B3, and located in the middle of the membrane. The question whether a significant amount of excitation energy proceeds via these two 'connecting' chlorophylls, which would imply that the chlorophylls eC-A2, eC-A3, eC-B2 and eC-B3 could be engaged both in excitation energy and in electron transfer, can not be answered at the moment. However, theoretical calculations, which have already been initiated, could provide a powerful tool to solve this problem.

7.2. The 'red' chlorophylls

In photosystem I there are chlorophylls which absorb at longer wavelength than P700 (so called 'long wavelength' or 'red' chlorophylls). Their number varies among different organisms [153,157,158]. PS I from *S. elongatus* contains nine to 11 Chl*a* per monomer which absorb light at longer wavelengths ('red shifted') than the bulk of antenna Chl*a* [157]. Two functional roles have been discussed for the 'red' chlorophylls: facilitation of efficient light energy capture under extreme environmental conditions, and focussing of the excitation energy to the reaction centre [113]. The red shift can be caused by several types of molecular interactions or properties of the chlorophylls: excitonic interaction of cofactors [159], deviations from planarity of the chlorine ring [160], charge effects [161], electronic interactions with polypeptide side chains, and changes in the dielectric constant of the local environment of the absorbing cofactors [162]. The structure at 2.5 Å resolution can not provide the final answer to the question of where the 'red' chlorophylls are located. However, tightly interacting chlorophylls, forming dimers and trimers of chlorophyll molecules, can be identified. These chlorophylls, which are most probably excitonically coupled, are possible candidates for some of the long wavelength chlorophylls. In the following, the discussion will focus on a unique Chl trimer and three Chl dimers located at prominent positions in the complex.

On the lumenal side of the membrane close to PsaX, a Chl*a* trimer formed by aC-B31, aC-B32 and aC-B33 is located. The arrangement of the three Chl*a* can be best described as a staircase, where the pigment molecules can be seen to be related to each other by an approximate translation, with their ring planes oriented roughly parallel (Fig. 9). The interplanar separations between the chlorophylls are in

the range from 3.5 to 3.7 Å, with lateral centre to centre shifts of 8.3 Å. Strong excitonic coupling is implied by this geometry of approximate translational symmetry, because the transition dipole moments of the chlorine rings are roughly parallel. PsaB coordinates only one of these three chlorophylls, aC-B31, directly via HisB470, whereas the Mg^{2+} ions of the other two Chl*a* molecules, aC-B32 and aC-B33, are coordinated to water molecules. It is remarkable, that the topography of this chlorophyll trimer is similar to small molecule crystal structures of chlorophyll derivatives [163], showing an absorption maximum at 740 nm within the crystals. For these chlorophyll derivatives, the extreme red shift compared to solutions was explained by strong excitonic interactions supported by π–π interactions within the stacks. Only one Chl*a* trimer is observed in the structure of PS I from *S. elongatus*. The cause of the lack of a chlorophyll trimer in PsaA at a position related by the pseudo-C_2 axis could be an interference of the hypothetical PsaA counterpart with the monomer-monomer contact within the trimer.

At the lumenal side of the membrane at the interface between PS I monomers, one pair consisting of chlorophylls aC-A32 and aC-B7 is located. These two chlorophylls are coloured red in Fig. 9. They are separated by a centre to centre distance of 8.9 Å and an interplanar distance of 3.5 Å. Hydrophobic contacts are observed between this pair of chlorophylls and the C-terminal region of PsaL from the adjacent monomer. In 1998, Palsson et al. detected a loss of two chlorophylls absorbing at 719 nm, when the trimer of *S. elongatus* was split into monomers [157]. Possibly, these two chlorophylls could be identical with the chlorophyll pair aC-A32/aC-B7. These chlorophylls could also play a role in excitation energy transfer between the monomers.

Two further Chl*a* dimers are located at prominent positions near the stromal side of the membrane, which are related to each other by the pseudo-C_2 symmetry. One dimer is constituted by aC-A38 and aC-A39, coordinated to PsaA, the other consists of ac-B37 and aC-B38 coordinated to PsaB. The dimer aC-A38/aC-A39 is located close to PsaF, aC-B37/aC-B38 close to PsaL. In contrast to the majority of the bulk chlorophylls, their chlorine head groups are oriented parallel to the membrane. The centre to centre distances within the pairs aC-A38/aC-A39 and aC-B37/aC-B38 are 8.2 Å and 7.6 Å, respectively. Their ring systems are stacked at 3.5 Å separation so that their π electron systems overlap partially. In close proximity to each of the two Chl*a* pairs, one of the 'connecting' Chl*a* is located; the centre to centre distances between aC-A38/aC-A39 and aC-A40 and aC-B37/aC-B38 and aC-B39 are about 16 Å. Based on geometrical considerations, we can speculate that the excitation energy transfer from these Chl*a* dimers to the ETC can be achieved at reasonable rates via the two 'connecting' chlorophylls, thereby suggesting that these two dimers as well as the 'connecting' chlorophylls may play a special role in excitation energy transfer.

7.3. The carotenoids

The complex organisation of antenna Chl*a* and carotenoids underlines two major functions besides a structural function in stabilisation of the PS I complex: light harvesting and photoprotection [164]. Carotenoids absorb at wavelengths different from that of Chl*a*, in the range 450–570 nm. Their photoprotective function is correlated to their ability to quench excited Chl*a* triplet states which can generate toxic singlet oxygen (for review see [165]). This function is of importance in vivo if the cells are overexposed to light. It is in agreement with the fact that cells lacking carotenoids are very sensitive to light [166].

In the electron density map at 2.5 Å resolution, 22 carotenoids have been identified and were modelled as β-carotene. This carotene has been previously shown to be the dominant carotenoid in PS I [24,167]. 17 carotenoids show the *all-trans* configuration, whereas the remaining five carotenes contain one or two *cis* bonds: two carotenes were modelled as *9-cis*, and one each as *9,9′-cis*, *9,13′-cis* and *13-cis* carotenoids, respectively. Previous HPLC analysis of PS I from *S. vulcanus* [164] reveals some but not all of the isomers which have been now identified in the structure.

The majority of the carotenoids are deeply inserted into the membrane, with only a few of the head groups located closer to the stromal or lumenal side. The carotenoids are arranged in six clusters (Fig. 9a). The clusters (1), (2), (3) and (4), contain three, three, two and two carotenoid molecules, re-

spectively. The carotenoids in these clusters form various hydrophobic contacts with PsaA and PsaB, with cluster (1) being additionally in contact with PsaK. The carotenoids in clusters (1) and (3) are roughly related by the pseudo-C_2 axis to those in clusters (2) and (4), respectively. Each of the clusters (5) and (6) contains six carotenoids. Cluster (5) is located at the distal side of the PsaA/B heterodimer as seen from the C_3 axis of the PS I trimer, whereas cluster (6) is located at the proximal side. The carotenoids in cluster (5) form hydrophobic interactions with PsaA and PsaB and PsaF and PsaJ, whereas the carotenoids of cluster (6) interact with PsaA, PsaB, PsaI, PsaL and PsaM. For these two clusters, the pseudo-C_2 symmetry is not well expressed.

Tight interactions can be observed between the carotenoids and the chlorophylls of the antenna system. Efficient energy transfer from excited carotenoids to the Chl*a* as well as quenching of Chl*a* triplets, which occurs via a charge transfer mechanism [168], depend on interactions between carotenoids and chlorophylls within the van der Waals contact. Indeed, all carotenoids are in direct vicinity to Chl*a* head groups (<3.6 Å). 60 out of the 90 antenna chlorophylls are in direct contact to carotenoids, thereby facilitating efficient triplet quenching and energy transfer. Furthermore, extended π–π stacking is observed for a few pairs of Chl*a* and carotenoids in the PS I structure. This kind of interactions could be important for the fine-tuning of the absorption properties of the antenna.

7.4. Lipids

In the 2.5 Å structure of PS I, four lipid molecules are identified. They are bound by PsaA/B. Three of them are negatively charged phospholipids (I, III, IV), whereas one of them is an uncharged galactolipid (II). Chemical (Linke et al., in preparation) and immunological investigations [169] identified these types of lipids in PS I from *S. elongatus* to be monogalactosyldiglyceride and phosphatidylglycerol. The lipids are located in the central core of PsaA and PsaB as previously suggested [169]. For all four lipids the head groups, forming bonds with PsaA/PsaB, are located at the stromal side of the membrane. The two fatty acid chains of each lipid are anchored between transmembrane α-helices of PsaA/PsaB and extend to the middle of the membrane. In addition, one antenna Chl*a*, aC-PL1, is coordinated by the phosphodiester group of lipid (III). The binding of the lipids seems to be an evolutionary conserved feature of PS I, because the lipids are related by the pseudo-C_2 axis: galactolipid (II) and phospholipid (I) are located close to the central core of the 10 transmembrane α-helices, A/B-g to A/B-k, surrounding the electron transfer chain. As discussed above, a possible influence of the uncharged lipid (II)/charged lipid (I) on the two phylloquinone binding sites Q_K-B and Q_K-A has to be considered. The other two lipids are situated more peripherally. Lipid (III) is bound to PsaA, located close to the monomer–monomer interface, whereas lipid (IV) is bound to PsaB, being in contact with PsaX. The location of lipids (I) and (II) close to the core of the PS I structure, and the obvious function of lipid (III) in binding of an antenna Chl*a*, clearly indicate that the four lipid molecules are integral and functionally important constituents of the PS I complex.

Acknowledgements

We thank Dr. Catherine Fursman and Jan Kern for the critical reading of the manuscript.

References

[1] J.H. Golbeck, in: D.A. Bryant (Ed.), Advances in Photosynthesis: The Molecular Biology of Cyanobacteria, Vol. 1, Kluwer Academic Publishers, Dordrecht, 1994, pp. 319–360.
[2] P.R. Chitnis, Plant Physiol. 111 (1996) 661–669.
[3] P. Jordan, P. Fromme, O. Klukas, H.T. Witt, W. Saenger, N. Krauß, Nature 411 (2001) 909–917.
[4] J. Hladik, D. Sofrova, Photosynth. Res. 29 (1991) 171–175.
[5] G. Döring, J.L. Bailey, J. Weikara, H.T. Witt, Naturwissenschaften 5 (1968) 219–224.
[6] J.R. Norris, R.A. Uphaus, H.L. Crespi, J.J. Katz, Proc. Natl. Acad. Sci. USA 68 (1971) 625–628.
[7] K. Brettel, Biochim. Biophys. Acta 1318 (1997) 322–373.
[8] R.E. Blankenship, Photosynth. Res. 33 (1992) 91–111.
[9] U. Feiler, G. Hauska, in: R.E. Blankenship, M.T. Madigan, C.F. Bauer (Eds.), Anoxygenic Photosynthetic Bacteria, Vol. 1, Kluwer Academic Publishers, London, 1995, pp. 665–685.
[10] W.D. Schubert, O. Klukas, W. Saenger, H.T. Witt, P. Fromme, N. Krauss, J. Mol. Biol. 280 (1998) 297–314.

[11] N. Krauss, W. Hinrichs, I. Witt, P. Fromme, W. Pritzkow, Z. Dauter, C. Betzel, K.S. Wilson, H.T. Witt, W. Saenger, Nature 361 (1993) 326–361.
[12] N. Krauss, W.D. Schubert, O. Klukas, P. Fromme, H.T. Witt, W. Saenger, Nat. Struct. Biol. 3 (1996) 965–973.
[13] O. Klukas, W.D. Schubert, P. Jordan, N. Krauss, P. Fromme, H.T. Witt, W. Saenger, J. Biol. Chem. 274 (1999) 7361–7367.
[14] O. Klukas, W.D. Schubert, P. Jordan, N. Krauss, P. Fromme, H.T. Witt, W. Saenger, J. Biol. Chem. 274 (1999) 7351–7360.
[15] W.D. Schubert, O. Klukas, N. Krauss, W. Saenger, P. Fromme, H.T. Witt, J. Mol. Biol. 272 (1997) 741–769.
[16] L. Fish, U. Kück, L. Bogorad, J. Biol. Chem. 260 (1985) 1413–1421.
[17] U. Mühlenhoff, W. Haehnel, H.T. Witt, R.G. Herrmann, Gene 127 (1993) 71–78.
[18] P. Fromme, W.-D. Schubert, N. Krauss, Biochim. Biophys. Acta 1187 (1994) 99–105.
[19] J. Sun, Q. Xu, V.P. Chitnis, P. Jin, P.R. Chitnis, J. Biol. Chem. 272 (1997) 21793–21802.
[20] Q. Xu, P.R. Chitnis, Plant Physiol. 108 (1995) 1067–1075.
[21] J. Deisenhofer, O. Epp, I. Sinning, H. Michel, J. Mol. Biol. 246 (1995) 429–457.
[22] K.H. Rhee, E.P. Morris, J. Barber, W. Kühlbrandt, Nature 396 (1998) 283–286.
[23] A. Zouni, H.T. Witt, J. Kern, P. Fromme, N. Krauß, W. Saenger, P. Orth, Nature 409 (2001) 739–743.
[24] A. Makewicz, A. Radunz, G.H. Schmidt, Z. Naturforsch. 51c (1996) 319–328.
[25] H. Hatanaka, K. Sonoike, M. Hirano, S. Katoh, Biochim. Biophys. Acta 1141 (1993) 45–51.
[26] Q. Xu, L. Yu, V.P. Chitnis, P.R. Chitnis, J. Biol. Chem. 269 (1994) 3205–3211.
[27] M. Hippler, J. Reichert, M. Sutter, E. Zak, L. Altschmied, U. Schroer, R.G. Herrmann, W. Haehnel, EMBO J. 15 (1996) 6374–6384.
[28] M. Hippler, F. Drepper, J.D. Rochaix, U. Mühlenhoff, J. Biol. Chem. 274 (1999) 4180–4188.
[29] J. Sun, W. Xu, M. Hervas, J.A. Navarro, M.A. Rosa, P.R. Chitnis, J. Biol. Chem. 274 (1999) 19048–19054.
[30] A.L. Zilber, R. Malkin, Plant Physiol. 99 (1992) 901–911.
[31] M.C.W. Evans, A. Telfer, A.V. Lord, Biochim. Biophys. Acta 267 (1972) 530–537.
[32] R. Cammak, M.C.W. Evans, Biochem. Biophys. Res. Commun. 67 (1975) 544–549.
[33] P.B. Hoj, I. Svendsen, H.V. Scheller, B.L. Moller, J. Biol. Chem. 262 (1987) 12676–12684.
[34] H. Oh-oka, Y. Takahashi, K. Kuriyama, K. Saeki, H. Matsubara, J. Biochem. (Tokyo) 103 (1988) 962–968.
[35] E.T. Adman, L.C. Sieker, L.H. Jensen, J. Biol. Chem. 248 (1973) 3987–3996.
[36] J.H. Golbeck, Plant Physiol. 111 (1996) 661–669.
[37] L. Yu, D.A. Brant, J.H. Golbeck, Biochemistry 34 (1995) 7861–7868.
[38] L. Yu, I.R. Vassiliev, Y.S. Jung, D.A. Bryant, J.H. Golbeck, J. Biol. Chem. 270 (1995) 28118–28125.
[39] N. Fischer, P. Setif, J.D. Rochaix, J. Biol. Chem. 274 (1999) 23333–23340.
[40] K.V. Lakshmi, Y.S. Jung, J.H. Golbeck, G.W. Brudvig, Biochemistry 38 (1999) 13210–13215.
[41] J.H. Golbeck, Photosynth. Res. 61 (1999) 107–144.
[42] G. Zanetti, G. Merati, Eur. J. Biochem. 169 (1987) 143–146.
[43] C. Lelong, E.J. Boekema, J. Kruip, H. Bottin, M. Rögner, P. Setif, EMBO J. 15 (1996) 2160–2168.
[44] U. Mühlenhoff, J. Zhao, D.A. Bryant, Eur. J. Biochem. 235 (1996) 324–331.
[45] V.P. Chitnis, Y.S. Jungs, L. Albee, J.H. Golbeck, P.R. Chitnis, J. Biol. Chem. 271 (1996) 11772–11780.
[46] V.P. Chitnis, A. Ke, P.R. Chitnis, Plant Physiol. 115 (1997) 1699–1705.
[47] P. Barth, B. Laoutte, P. Setif, Biochemistry 37 (1998) 16233–16241.
[48] V. Pandini, A. Aliverti, G. Zanetti, Biochemistry 38 (1999) 10707–10713.
[49] Z. Xia, R.W. Broadhurst, E.D. Laue, D.A. Bryant, J.H. Golbeck, D.S. Bendall, Eur. J. Biochem. 255 (1998) 309–316.
[50] J. Golbeck, Curr. Opin. Struct. Biol. 3 (1992) 508–514.
[51] N. Li, J.D. Zhao, P.V. Warren, J.T. Warden, D.A. Bryant, J.H. Golbeck, Biochemistry 30 (1991) 7863–7872.
[52] Q. Xu, T.S. Armbrust, J.A. Guikema, P.R. Chitnis, Plant. Physiol. 106 (1994) 1057–1063.
[53] S. Janson, B. Andersen, H.V. Scheller, Plant Physiol. 112 (1996) 409–420.
[54] T.S. Armbrust, P.R. Chitnis, J.A. Guikema, Plant Physiol. 111 (1996) 1307–1312.
[55] Q. Xu, J.A. Guikema, P.R. Chitnis, Plant Physiol. 106 (1994) 617–624.
[56] K. Sonoike, H. Hatanaka, S. Katoh, Biochim. Biophys. Acta 1141 (1993) 52–57.
[57] N. Weber, H. Strotmann, Biochim. Biophys. Acta 1143 (1993) 204–210.
[58] F. Rousseau, P. Setif, B. Lagoutte, EMBO J. 12 (1993) 1755–1765.
[59] J. Zhao, W.B. Snyder, U. Mühlenhoff, E. Rhiel, P.V. Warren, J.H. Golbeck, D.A. Bryant, Mol. Microbiol. 9 (1993) 183–194.
[60] B. Andersen, H.V. Scheller, B.L. Moller, FEBS Lett. 311 (1992) 169–173.
[61] J. Kruip, P.R. Chitnis, B. Lagoutte, M. Rögner, E.J. Boekema, J. Biol. Chem. 272 (1997) 17061–17069.
[62] C.J. Falzone, Y.H. Kao, J. Zhao, D.A. Bryant, J.T. Lecomte, Biochemistry 33 (1994) 6052–6062.
[63] K. Meimberg, B. Lagoutte, H. Bottin, U. Mühlenhoff, Biochemistry 37 (1998) 9759–9767.
[64] J.J. van Thor, T.H. Geerlings, H.C. Matthijs, K.J. Hellingwerf, Biochemistry 38 (1999) 12735–12746.
[65] Q. Xu, Y.S. Jung, V.P. Chitnis, J.A. Guikema, J.H. Golbeck, P.R. Chitnis, J. Biol. Chem. 269 (1994) 21512–21518.
[66] U. Mühlenhoff, P. Setif, Biochemistry 35 (1996) 1367–1374.
[67] V.P. Chitnis, Q. Xu, L. Yu, J.H. Golbeck, H. Nakamoto,

D.-L. Xie, P.R. Chitnis, J. Biol. Chem. 268 (1993) 11678–11684.
[68] W.M. Schluchter, G. Shen, J. Zhao, D.A. Bryant, Photochem. Photobiol. 64 (1996) 53–66.
[69] Q. Xu, D. Hoppe, V.P. Chitnis, W.R. Odom, J.A. Guikema, P.R. Chitnis, J. Biol. Chem. 270 (1995) 16243–16250.
[70] B. Andersen, H.V. Scheller, in: C. Sundquist (Ed.), Plastids: Synthesis and Assembly, Academic Press, San Diego, CA, 1993, pp. 383–418.
[71] U. Mühlenhoff, F. Chauvat, Mol. Gen. Genet. 252 (1996) 93–100.
[72] P. Fromme, in: Habilitationsschrift Max Volmer Institute, Technical University Berlin, Berlin, 1998.
[73] N.V. Karapetyan, A.R. Holzwarth, M. Rögner, FEBS Lett. 460 (1999) 395–400.
[74] K. Ohyama, H. Fukazawa, T. Kohchi, H. Shirai, S. Tohru, S. Sano, K. Umesono, Y. Shiki, M. Takeuchi, Z. Chang, S.I. Aota, H. Inokuchi, H. Ozeki, Nature 322 (1986) 572–574.
[75] I. Karnauchov, D. Cai, I. Schmidt, R.G. Herrmann, R.B. Klosgen, J. Biol. Chem. 269 (1994) 32871–32878.
[76] M.P. Scott, V.S. Nielsen, J. Knoetzel, R. Andersen, B.L. Moller, Plant Mol. Biol. 26 (1994) 1223–1229.
[77] M. Hugosson, G. Nurani, E. Glaser, L.G. Franzen, Plant Mol. Biol. 28 (1995) 525–535.
[78] P.R. Chitnis, Q. Xu, V.P. Chitnis, R. Nechustai, Photosynth. Res. 44 (1995) 23–40.
[79] C. Bengis, N. Nelson, J. Biol. Chem. 252 (1977) 4564–4569.
[80] P.R. Chitnis, D. Purvis, N. Nelson, J. Biol. Chem. 266 (1991) 20146–20151.
[81] W. Haehnel, T. Janse, K. Gause, R.B. Klosgen, B. Stahl, D. Michl, B. Huvermann, M. Karas, R.G. Herrmann, EMBO J. 13 (1994) 1028–1038.
[82] J. Farah, F. Rappaport, Y. Choquet, P. Joliot, J.D. Rochaix, EMBO J. 14 (1995) 4976–4984.
[83] M. Hippler, F. Drepper, J. Farah, J.D. Rochaix, Biochemistry 36 (1997) 6343–6349.
[84] M. Hippler, F. Drepper, W. Haehnel, J.D. Rochaix, Proc. Natl. Acad. Sci. USA 95 (1998) 7339–7344.
[85] N. Fischer, E. Boudreau, M. Hippler, F. Drepper, W. Haehnel, J.D. Rochaix, Biochemistry 38 (1999) 5546–5552.
[86] S. Anandan, A. Vainstein, J.P. Thornber, FEBS Lett. 256 (1989) 150–154.
[87] Q. Xu, W.R. Odom, J.A. Guikema, V.P. Chitnis, P.R. Chitnis, Plant Mol. Biol. 26 (1994) 291–302.
[88] K. Koike, M. Ikeuchi, T. Hiyama, Y. Inoue, FEBS Lett. 253 (1989) 257–263.
[89] M. Ikeuchi, K.J. Nyhus, Y. Inoue, H.B. Pakrasi, FEBS Lett. 287 (1991) 5–9.
[90] Y. Gavel, J. Steppuhn, R. Herrmann, G. von Heijne, FEBS Lett. 282 (1991) 41–46.
[91] S. Kjaerulff, B. Andersen, V.S. Nielsen, B.L. Moller, J.S. Okkels, J. Biol. Chem. 268 (1993) 18912–18916.
[92] W. Nitschke, A.W. Rutherford, Trends Biochem. Sci. 16 (1991) 241–245.
[93] U. Ermler, H. Michel, M. Schiffer, J. Bioenerg. Biomembr. 26 (1994) 5–15.
[94] G. Trinkunas, A.R. Holzwarth, Biophys. J. 71 (1996) 351–364.
[95] P. Setif, in: J. Barber (Ed.), The Photosystems: Structure, Function and Molecular Biology, Elsevier Science Publishers, Amsterdam, 1992.
[96] P. Moenne-Loccoz, B. Robert, I. Ikegami, M. Lutz, Biochemistry 29 (1990) 4740–4746.
[97] I. Sieckmann, K. Brettel, C. Bock, A. van der Est, D. Stehlik, Biochemistry 32 (1993) 4842–4847.
[98] E. Hamacher, J. Kruip, M. Rögner, W. Mäntele, in: P. Mathis (Ed.), Photosynthesis: From Light to Biosphere, Vol. III, Kluwer Academic Publishers, London, 1995, pp. 95–98.
[99] H. Käß, E. Bittersmann-Weidlich, L.-E. Andreasson, B. Boenigk, W. Lubitz, Chem. Phys. 194 (1995) 419–432.
[100] H. Käß, Thesis, Technical University Berlin, Berlin, 1995.
[101] H. Käß, P. Fromme, H.T. Witt, W. Lubitz, J. Phys. Chem. B 105 (2001) 1225–1239.
[102] M. Mac, X.S. Tang, B.A. Diner, J. McCracken, G.T. Babcock, Biochemistry 35 (1996) 13288–13293.
[103] K. Redding, F. MacMillan, W. Leibl, K. Brettel, J. Hanley, A.W. Rutherford, J. Breton, J.D. Rochaix, EMBO J. 17 (1998) 50–60.
[104] A.N. Webber, H. Su, S.E. Bingham, H. Käß, L. Krabben, M. Kuhn, R. Jordan, E. Schlodder, W. Lubitz, Biochemistry 35 (1996) 12857–12863.
[105] A.N. Melkozernov, H. Su, S. Lin, S. Bingham, A.N. Webber, R.E. Blankenship, Biochemistry 36 (1997) 2898–2907.
[106] T. Watanabe, M. Kobayashi, A. Hongu, M. Nakazato, T. Hiyama, FEBS Lett. 235 (1985) 252–256.
[107] H. Maeda, T. Watanabe, M. Kobayashi, I. Ikegami, Biochim. Biophys. Acta 1099 (1992) 74–80.
[108] J. Maroc, A. Tremolieres, Biochim. Biophys. Acta 1018 (1990) 67–71.
[109] K. Artz, J.C. Williams, J.P. Allen, F. Lendzian, J. Rautter, W. Lubitz, Proc. Natl. Acad. Sci. USA 94 (1997) 13582–13587.
[110] B. Hecks, K. Wulf, J. Breton, W. Leibl, H.-W. Trissl, Biochemistry 33 (1994) 8619–8624.
[111] S. Kumazaki, H. Kandori, H. Petek, K. Yoshihara, I. Ikegami, J. Phys. Chem. 98 (1994) 10335–10342.
[112] G. Trinkunas, A.R. Holzwarth, Biophys. J. 66 (1994) 415–429.
[113] R. van Grondelle, J. Dekker, T. Gillbro, V. Sundström, Biochim. Biophys. Acta 1187 (1994) 1–65.
[114] R.W. Mansfield, M.C.W. Evans, FEBS Lett. 190 (1985) 237–241.
[115] U. Ermler, G. Fritzsch, S.K. Buchanan, H. Michel, Structure 2 (1994) 925–936.
[116] G. Hastings, S. Hoshina, A.N. Webber, R.E. Blankenship, Biochemistry 34 (1995) 15512–15522.
[117] W. Zinth, T. Arlt, J. Wachveitl, Ber. Bunsenges. Phys. Chem. 100 (1996) 1962–1966.

[118] M. Iwaki, S. Kumazaki, K. Yoshihara, T. Erabi, S. Itoh, J. Phys. Chem. 100 (1996) 10802–10809.
[119] C.C. Moser, P.L. Dutton, Biochim. Biophys. Acta 1101 (1992) 171–176.
[120] R. Malkin, FEBS Lett. 208 (1986) 343–346.
[121] J. Biggins, P. Mathis, Biochemistry 27 (1988) 1494–1500.
[122] T. Schwartz, K. Brettel, in: P. Mathis (Ed.), Photosynthesis: From Light to Bioshpere, Vol. II, Kluwer Academic Publishers, Amsterdam, 1995, pp. 119–122.
[123] F. MacMillan, J. Hanley, L. van der Weerd, M. Knupling, S. Un, A.W. Rutherford, Biochemistry 36 (1997) 9297–9303.
[124] A. Kamlowski, S.G. Zech, P. Fromme, R. Bittl, W. Lubitz, H.T. Witt, D. Stehlik, J. Phys. Chem. 102 (1998) 8266–8277.
[125] R. Bittl, S.G. Zech, P. Fromme, H.T. Witt, W. Lubitz, Biochemistry 36 (1997) 12001–12004.
[126] S.A. Dzuba, P. Gast, A.J. Hoff, Chem. Phys. Lett. 235 (1997) 595–602.
[127] A. Kamlowksi, B. Altenberg-Greulich, A. van der Est, S.G. Zech, R. Bittl, P. Fromme, W. Lubitz, D. Stehlik, J. Phys. Chem. B 102 (1998) 8278–8287.
[128] M. Iwaki, S. Itoh, Biochemistry 30 (1991) 5347–5352.
[129] S.E.J. Rigby, M.C.W. Evans, P. Heathcote, Biochemistry 35 (1996) 6651–6656.
[130] D. Xia, C.-A. Yu, H. Kim, J.-Z. Xia, A.M. Kachurin, L. Zhang, L. Yu, J. Deisenhofer, Science 277 (1997) 60–66.
[131] J. Abramson, S. Riistama, G. Larsson, A. Jasaitis, M. Svensson-Ek, L. Laakkonen, A. Puustinen, S. Iwata, M. Wikstrom, Nat. Struct. Biol. 7 (2000) 910–917.
[132] S. Iwata, C. Ostermeier, B. Ludwig, H. Michel, Nature 376 (1995) 660–669.
[133] M. Iwata, K. Okada, S. Iwata, Tanpakushitsu Kakusan Koso 44 (1999) 643–654.
[134] Z. Zhang, L. Huang, V.M. Shulmeister, Y.I. Chi, K.K. Kim, L.W. Hung, A.R. Crofts, E.A. Berry, S.H. Kim, Nature 392 (1998) 677–684.
[135] F. Yang, G. Shen, W.M. Schluchter, B.L. Zybailov, A.O. Ganago, I.R. Vassiliev, D.A. Bryant, J.H. Golbeck, J. Phys. Chem. B 102 (1998) 8288–8299.
[136] P. Setif, K. Brettel, Biochemistry 32 (1993) 7846–7854.
[137] E. Schlodder, K. Falkenberg, M. Gergeleit, K. Brettel, Biochemistry 37 (1998) 9466–9476.
[138] P. Joliot, A. Joliot, Biochemistry 38 (1999) 11130–11136.
[139] M. Guergova-Kuras, B. Boudreaux, P. Joliot, K. Redding, Proc. Natl. Acad. Sci. USA 98 (2001) 4437–4442.
[140] B. Hallahan, S. Purton, A. Ivison, D. Wright, M.C.W. Evans, Photosynth. Res. 46 (1995) 257–264.
[141] I.R. Vassiliev, Y.S. Jung, L.B. Smart, R. Schulz, L. McIntosh, J.H. Golbeck, Biophys. J. 69 (1995) 1544–1553.
[142] W. Leibl, B. Toupance, J. Breton, EMBO J. 15 (1995) 101–109.
[143] A. van der Est, C. Bock, J. Golbeck, K. Brettel, P. Setif, D. Stehlik, Biochemistry 33 (1994) 11789–11797.
[144] J. Lüneberg, P. Fromme, P. Jekow, E. Schlodder, FEBS Lett. 338 (1994) 197–202.
[145] J.E. Franke, L. Ciesla, J.T. Warden, in: P. Mathis (Ed.), Photosynthesis: From Light to Biosphere, Vol. II, Kluwer Academic Publishers, Amsterdam, 1995, pp. 75–78.
[146] P. Setif, H. Bottin, Biochemistry 34 (1995) 9059–9070.
[147] G. McDermott, S.M. Prince, A.A. Freer, A.M. Hawthornthwaite-Lawless, M.Z. Papiz, R.J. Cogdell, N.W. Isaacs, Nature 374 (1995) 517–521.
[148] S. Karrasch, P.A. Bullough, R. Ghosh, EMBO J. 14 (1995) 631–638.
[149] H. Frank, R.J. Cogdell, Photochem. Photobiol. 63 (1995) 257–264.
[150] T.G. Owens, S.P. Webb, R.S. Alberte, L. Mets, G.R. Fleming, Biophys. J. 53 (1988) 733–745.
[151] M. Werst, Y. Jia, L. Mets, G.R. Fleming, Biophys. J. 61 (1992) 868–878.
[152] S. Savikhin, W. Xu, V. Soukoulis, P.R. Chitnis, W.S. Struve, Biophys. J. 76 (1999) 3278–3288.
[153] A.N. Melkozernov, S. Lin, R.E. Blankenship, Biochemistry 39 (2000) 1489–1498.
[154] L. DiMagno, C.K. Chan, Y. Jia, M.J. Lang, J.R. Newman, L. Mets, G.R. Fleming, R. Haselkorn, Proc. Natl. Acad. Sci. USA 92 (1995) 2715–2719.
[155] L. Valkunas, V. Liuolia, J.P. Dekker, R. van Grondelle, Photosynth. Res. 43 (1995) 149–154.
[156] T. Förster, Ann. Phys. (Leipzig) 2 (1948) 55–75.
[157] L.O. Pålsson, C. Flemming, B. Gobets, R. van Grondelle, J.P. Dekker, E. Schlodder, Biophys. J. 74 (1998) 2611–2622.
[158] V.V. Shubin, I.N. Bezsmertnaya, N.V. Karapetyan, FEBS Lett. 309 (1992) 340–342.
[159] V. Sundström, R. van Grondelle, in: R.E. Blankenship, M.T. Madigan, C.E. Bauer (Eds.), Anoxygenic Photosynthetic Bacteria, Vol. 1, Kluwer Academic Publishers, Amsterdam, 1995, pp. 349–372.
[160] E. Gudowska-Nowak, M.D. Newton, J. Fajer, J. Phys. Chem. 94 (1990) 5795–5801.
[161] J. Eccles, B. Honig, Proc. Natl. Acad. Sci. USA 80 (1983) 4959–4962.
[162] R.B. Altmann, I. Renge, L. Kador, D. Haarer, J. Chem. Phys. 97 (1992) 5316–5322.
[163] C. Kratky, J.D. Dunitz, J. Mol. Biol. 113 (1977) 431–442.
[164] G.E. Bialek-Bylka, E. Grazyna, R. Fujii, C.-H. Chen, H. Oh-Oka, A. Kamiesu, K. Satoh, H. Koike, Y. Koyama, Photosynth. Res. 58 (1998) 135–142.
[165] R.J. Cogdell, Pure Appl. Chem. 57 (1985) 723–728.
[166] S. Roemer, H. Senger, N.I. Bishop, Bot. Acta 108 (1995) 80–86.
[167] J. Coufal, J. Hladik, D. Sofrova, Photosynthetica 23 (1989) 603–616.
[168] D.L. Dexter, J. Chem. Phys. 21 (1953) 836–850.
[169] A. Makewicz, A. Radunz, G.H. Schmidt, in: J.-C. Kader, P. Mazliak (Eds.), Plant Lipid Metabolism, Kluwer Academic Publishers, Dordrecht, 1995, pp. 156–160.